

The authors thank the reviewers for their positive feedbacks on our work and their helpful comments and questions. We have addressed all comments and corrections as detailed below, and we modified the manuscript accordingly (all changes are highlighted in yellow in the version you can find below).

REVIEWER 1

Major comment

My only major comment is regarding the ability of the SAR to be extrapolated to a wider spectrum of compounds.

Although a narrow number of experimental data were used to build this SAR, we carefully chose monofunctional compounds and polyfunctional compounds in the extrapolation bearing the same chemical functions. Further arguments are also developed below.

The linear relationship shown in Fig 6 is between the SAR-simulated values and the experimental values from which the SAR was derived; correct?

Figure 6 plots all experimental k_{OH} values against the simulated k_{OH} values for the compounds which were used for the SAR construction. The data are compared to the 1:1 regression (plain line). The linear regression between the two sets is not shown for clarity.

For more clarity, we replaced the sentence in line 396 “Figure 6 shows the correlation between the calculated and the experimental rate constants showing a good linearity” by “Figure 6 shows the correlation between the calculated versus the experimental k_{OH} values, and it is compared to the 1:1 regression line.”

For other empirically-derived relationships, such as free energy linear relationships (LFERs), it is important to derive the relationship with a training set, followed by validation using an experimental set. With the limited number of organic nitrates, this may be challenging. What about ethers? Either way, the authors should comment on the reliability of the SAR when used for other compounds.

The SAR was firstly developed by Monod and Doussin (2008) for alkanes, cyclic compounds, alcohols, carboxylic acids and carboxylates and was then developed for ketones and aldehydes by Doussin and Monod (2013). We have extended the SAR to include organic nitrates and ethers by adding 4 parameters to the SAR. Those new parameters were varied while all the previous parameters remained unchanged.

For ethers, 34 k_{OH} experimental values (including 8 cyclic ethers) were used to resolve 3 different variables ($F(-O-)$, $G(-O-)$ and $X(-O-)$). In the case of $RONO_2$, the dataset was more limited: 7 k_{OH} values were used to resolve one variable ($F(-ONO_2)=G(-ONO_2)$). For this type of relationships, it is usually considered that a ratio of at least 10 experimental values for 1 variable is a rule to follow to avoid overfitting the SAR (Peduzzi et al., 1996). The approach to use a training set and then validate the results with a different set may be done only with a sufficiently large dataset. Therefore, we decided to use all the available experimental data to have the ‘best possible’ training set. Meanwhile, there are some aspects in our approach and in the results that can provide some validation:

- 1) One aspect concerns the validation of preexisting SAR parameters. Only four new parameters were added in this extended SAR, while the preexisting 26 parameters remained unchanged. Considering that the extension of the SAR with four additional parameters did not require any optimization of the preexisting parameters, we can consider that the new experimental data act as validation of these preexisting parameters.
- 2) This SAR extension incorporates, in respect to the previous developed SAR, the weighting of the experimental values with their uncertainties. A k_{OH} value with a lower uncertainty was thus more constraining than values with higher (or no) uncertainties. This improvement of the approach renders

difficult the sorting of data to build a ‘training set’ and a ‘validation set’. On one hand, not using the data with low uncertainties for the SAR construction may induce significant deviations in the resulting SAR parameters. On the other hand, using data with high uncertainties for the validation cannot be completely trusted. In our approach, all experimental values were included in the training set, thus data bearing low uncertainties had a higher influence on the determined parameters. The fact that only a few significant discrepancies (deviations by a factor of 2) between the experimental and simulated values even for low-weighted experimental values gives some validation of the final parameters.

3) Furthermore, the facts that the resolved parameters were chemically coherent, and that a wide range of reactivities was covered (two orders of magnitude), provide evidence to rely on the application of the extended SAR to other compounds.

4) A third aspect concerns isosorbide 5-mononitrate that can provide some validation of our SAR: this molecule presents a highly complex polyfunctional structure, with 2 ethers, 2 cycles, one alcohol and one nitrate group. The fact that its simulated k_{OH} value ($14.2 \times 10^8 \text{ L mol}^{-1} \text{ s}^{-1}$) agrees (within uncertainties) with the experimental value ($18 (\pm 5) \times 10^8 \text{ L mol}^{-1} \text{ s}^{-1}$) gives some validation of the extended SAR application to polyfunctional compounds.

We have modified the manuscript highlighting that i) the good results obtained even for the low-weighted values, ii) the chemical coherence of the resulting SAR parameters, iii) the large range of k_{OH} values covered by the data, and that iv) some validation can be done using isosorbide 5-mononitrate.

In line 397: “It shows a good linearity covering a wide range of reactivities (two orders of magnitude).”

In line 405: “Several arguments provide some evidence on the reliability of the application of the SAR to other compounds: i) there are only a few discrepancies (deviations by a factor of 2) between the experimental and simulated values, even for low-weighted experimental values, ii) the resolved parameters were chemically coherent, iii) a wide range of reactivities was covered (two orders of magnitude) and iv) isosorbide 5-mononitrate presents a highly complex polyfunctional structure (two cycles, two ether, one alcohol and one nitrate groups), the good agreement between its simulated and experimental k_{OH} values (within uncertainties, Table 2) gives some validation of the extended SAR application to polyfunctional compounds.”

Minor comments

Can any of the secondary organic nitrates used in the experiment undergo hydrolysis within the time scale of the experiment? Maybe this is confirmed with the H₂O₂ control experiment?

In addition to the H₂O₂ control experiments, control experiments were performed at pH = 2–3 for all organic nitrates within the time scale of the experiments. None of them showed any decay due to reaction with H₂O₂ or hydrolysis of the nitrate group, and we verified that none of them showed any formation of NO₃[–], product of organic nitrates hydrolysis (Darer et al., 2011).

We added in the manuscript, in line 115: “Furthermore, control experiments at pH = 2.5 confirmed that none of the organic nitrates underwent hydrolysis at significant rates under our experimental conditions.”

My understanding is that Figure 7 represents the phase partitioning of these species in equilibrium. Two minor questions:

Is partitioning equilibrium achieved in the atmosphere? Maybe yes for cloudwater, how about aerosol liquid water (e.g., viscosity)

We agree with Reviewer 1 on that point: in their kinetic flux model Shiraiwa and Seinfeld (2012) demonstrate that equilibrium is achieved in the order of seconds or minutes for the phase partitioning of relatively high volatility organic compounds into liquid particles, while the equilibration timescale

ranges from hours to days for semi-solid viscous particles, low volatility species or large particle sizes, and thus can be subject to equilibrium shifts by faster chemical reactions in each phase. However, these considerations are beyond the scope of our manuscript. Our goal is to show how aqueous-phase chemistry can affect organic nitrate fate even at very low LWC. To do so, we consider a very simple model of deliquescent particles containing a LWC of $3.5 \cdot 10^{-5}$ g m⁻³, and assuming fast phase partitioning.

We have added a sentence explaining this assumption in the manuscript:

In line 458: "It is worth noting that in the atmosphere, the equilibrium may not be instantaneous. In their kinetic flux model, Shiraiwa and Seinfeld (2012) demonstrate that equilibrium is achieved in the order of seconds or minutes for the phase partitioning of relatively high volatility organic compounds into liquid particles, while the equilibration timescale ranges from hours to days for semi-solid viscous particles, low volatility species or large particle sizes, and thus can be subject to equilibrium shifts by faster chemical reactions in each phase. However, these considerations are beyond the scope of the study, as the goal was to determine how aqueous-phase chemistry can affect organic nitrates fate even at very low LWC. Thus, Eq. (12) was used to understand if the partition into the aerosol-phase is important compared to the aqueous-phase and the gas-phase, under the two investigated conditions."

Can some of the organic nitrate be surface active and partition to the air-water interface?

To our knowledge, there is no study on the role of organic nitrates as surfactants. Compounds with a significant surface activity present a polar group on one side and a saturated long carbon chain on the other. None of the organic nitrates presented in this work shows such a structure, except, perhaps, for 2-ethylhexyl nitrate. This may be the reason for the lack of solubility observed for this compound in our experiments.

- Line 466, how did the authors consider the reactivities of carboxylic acid and carboxylate? Is this parameterized in the previous version of SAR?

Yes. Parameters from Monod and Doussin (2008) were used to determine the $k_{OH,aq}$ of carboxylic acids and their conjugated bases.

To make clearer how $k_{OH,aq}$ values were calculated the manuscript was modified as follows:

In line 487: "The $k_{OH,aq}$ rate constants were calculated using the extended SAR developed in this work (Eq. (6)). Neighboring factors for nitrate and ether groups were those calculated in this work (Table 4) while all other parameters were taken from Doussin and Monod, (2013) and Monod and Doussin (2008). Eq. (8) was employed for compounds containing carbonyl groups. For organic nitrates containing a carboxylic acid functional group, the contributions of both the protonated molecule and its conjugated base were considered."

Technical Comments

- Line 283, the sentence, "indicating a likely solvent kinetic effect which lowers more effectively the reaction." is awkward. Maybe consider rephrasing to "implying a solvent kinetic effect that can more effectively suppress the reactivity"?

This has been modified as proposed, except for that we kept "lower" instead of "suppress".

- In a few places "prior" should be "prior to" E.g., "Prior to each experiment." Check lines 114, 154, 161, 193

This has been modified as proposed.

REVIEWER 2

»Major points«

The manuscript text is overall fine, but would be strengthened if unnecessary portions were removed (e.g., the discussion of the “direct method” to determine rate constants on lines 60 - 63), repetition was eliminated (e.g., lines 291-292 repeat lines 286-288), and the text was edited for issues such as noun-verb agreement (e.g., “Measurement were performed. . .” on line 178). In addition, using parentheses to try to put the opposite case inside of a sentence makes for difficult reading, e.g., line 516: “For molecules which partition to the aqueous-phase, a positive (respectively negative) value of indicates that the aqueous-phase reactivity increases (respectively decreases) the atmospheric loss of the molecule.” This should be revised.

Modifications were done to correct mistakes, repetitions of sentences and to clarify confusing sentences.

There are some issues with pH. First, the solution is listed as "pH < 3" (line 109), but the value should be closer to pH 2 since solutions contained 5 mM H₂SO₄ (line 764). This should be clarified. Second, I appreciate that an acidic solution is needed to keep Fe dissolved, but pH 2 is not relevant for most atmospheric waters, which are much less acidic. The low pH values used in the experiments are a bit concerning since past work has shown that the OH rate constant is sometimes pH dependent for classes of compounds that do not have a change in acid-base speciation across the pH range (e.g., Kroflic et al., PCCP, DOI: 10.1039/c9cp05533a).

A pH < 3 is needed to produce ·OH radicals by the Fenton reaction (Neyens and Baeyens, 2003). The manuscript has been modified to specify that all experiments were performed at pH = 2.5 as directly measured (Micro pH electrode, Thermo).

Compounds with a pH-dependent relation discussed in (Kroflič et al., 2020) are phenol and catechol. For these molecules, the ·OH radical adds to a double bond of the aromatic ring and forms an intermediate adduct. In this type of reaction, Smith et al., (2015) (referring to Ashton et al., (1995), Heath and Valsaraj, (2015) and Land and Ebert, (1967)) have hypothesized that the intermediate adducts lifetimes might decrease by the effect of the acidity or the high ionic strength at pH 2 (relative to pH 5). Among our set of organic nitrates, none of them contains any double carbon bond, thus their ·OH-oxidation likely proceeds via H-abstractions, without any intermediate adduct. For species undergoing H abstraction, the Fenton reaction has already been employed to determine k_{OH} values without significant discrepancies with studies performed at higher pH (e.g.: Buxton et al., (1988) and Herrmann et al., (2010)). This fact was also validated in this work by the determination of isopropanol and acetone k_{OH} values.

This was added to the manuscript in line 110: “pH = 2.5 (Micro pH electrode, Thermo)”

Third, the SAR lumps the current rate constants with 32 literature values without any tabulation or discussion of the pH values for the literature results. It's likely they were not done at pH 2, so it's not clear they can be considered along with the organic nitrates studied in this work. This should be examined and discussed.

The SAR only includes compounds reacting with ·OH by H-abstraction at various pH values. For the reason mentioned above, we consider that their experimental values can be used together.

The 2-ethylhexyl nitrate kinetic data looks suspicious (Figure 4) and produce a rate constant that is lower than expected and not included in the SAR (line 345). The authors (line 278) suggest that the experiments might have suffered from solubility issues, but they don't test this. As it currently stands, this compound is thus in publication purgatory: the data is reported in the manuscript,

but is not trusted. The authors need to take a stand on the compound, either (1) eliminate it entirely from the manuscript or (2) do additional experiments (e.g., at a lower concentration) to try to get good data.

To perform additional experiments at lower concentrations where 2-ethylhexyl nitrate would be completely dissolved in water would mean to work at concentrations around $10^{-6} - 10^{-7}$ M. This would suppose further uncertainties due to experimental difficulties e.g.: concentrations close to the detection limits of the analyzers. Furthermore, as mentioned in our response to Reviewer 1, from the molecular structure of 2-ethylhexyl nitrate, we suspect this molecule to present some surface activity. In this case, 2-ethylhexyl nitrate would remain at the water-air interface, thus preventing from complete dilution at any concentration. A specific experimental protocol would thus have to be deployed, but this is beyond the scope of this study. For these reasons, we did not perform any additional experiment, and, as suggested, we have discarded its kinetic data and removed it from all figures and tables. However, we would rather not eliminate all mention of this compound in the manuscript to report the limitations likely due to surface activity. Furthermore, to our knowledge this compound has never been investigated before for PTR-MS measurements, thus we want to provide this new data.

In line 273: "Data for 2-ethylhexyl nitrate showed inconsistency compared to the other alkyl nitrates (significantly lower value in respect to its chemical structure). It is possible that even with a low initial concentration ($5 \cdot 10^{-5}$ mol L⁻¹), well below its solubility threshold ($1 \cdot 10^{-4}$ mol L⁻¹) the complete dissolution of the compound was not achieved when the reaction started, thus inducing an incorrect rate constant value. Furthermore, it is suspected, from its structure, to present some surface activity, thus preventing this compound to dissolve into the bulk water."

The calculation and discussion of the lifetimes of the organic nitrates should be improved. (a) Fates other than OH (gas and aqueous) need to be better described. There is little discussion of hydrolysis, mostly just three lines about the rapid hydrolysis of compounds with the nitrate group on a tertiary carbon (lines 506-510). But don't other nitrates also have significant hydrolysis rate constants? This should be described and quantified.

To our knowledge the hydrolysis of the nitrate group is extremely structure dependent, mostly occurring for tertiary or allylic organic nitrates (Darer et al., 2011; Jacobs et al., 2014). It is an acid-catalyzed nucleophilic substitution unimolecular reaction (SN1) where the nitrate group is firstly protonated and after its elimination, a molecule of water attacks the carbocation leading to the formation of an alcohol and nitric acid (Rindelaub et al., 2016). The formation of α - and β -pinene particulate organic nitrates has been extensively studied in simulation chambers, showing that the non-hydrolyzable fraction ranges from 68 to 91 % in mass (Takeuchi and Ng, 2019). As mentioned in our answer to Reviewer 1, in our study, control experiments were performed at pH = 2.5 for all organic nitrates within the time scale of the experiments. None of them showed any decay due to reaction with H₂O₂ or hydrolysis of the nitrate group, and we verified that none of them showed the formation of NO₃⁻.

We added in the manuscript, in line 115: "Furthermore, control experiments at pH = 2.5 confirmed that none of the organic nitrates underwent hydrolysis at significant rates under our experimental conditions."

In addition, isn't photolysis (in both phases) a significant sink for some of the nitrates with an aldehyde or ketone group? This should be discussed, especially in terms of how these other fates would alter the lifetimes that are presented.

Photolysis is a likely sink for organic nitrates, mostly for carbonyl nitrates. Gas-phase photolysis lifetimes have been experimentally determined or simulated for eleven of these compounds and they range from 0.5 to 15 h (Barnes et al., 1993; Müller et al., 2014; Picquet-Varrault et al., 2020; Suarez-Bertoá et al., 2012). At these rates, gas-phase photolysis is expected to be the main chemical loss process for low molecular-weight carbonyl nitrates. On the other hand, to our knowledge, no aqueous-phase

photolysis lifetimes have been experimentally determined for carbonyl nitrates. Meanwhile, Romonosky et al. (2015) investigated molar absorptivity of a series of β -hydroxynitrates in the aqueous-phase, and, assuming similar quantum yields as in the gas-phase, they calculated the photolysis rate constant ratios between the gas- and aqueous-phase. Using their approach, aqueous phase photolysis is likely a major sink for water soluble carbonyl nitrates as it likely occurs for most isoprene-derived nitrates. However, their results show that $\cdot\text{OH}$ -oxidation in the aqueous- or the gas-phase is a more significant loss process than photolysis for β -hydroxynitrates. This could be the case for atmospherically relevant species such as C₅ dihydroxy dinitrate or for terpene nitrates. For the latter, their $\cdot\text{OH}$ -oxidation lifetimes fall in the same range as the photolysis lifetimes reported for carbonyl nitrates in the gas-phase thus both processes may be relevant for terpene nitrates and those containing carbonyl groups, but further experimental studies would deserve attention to confirm this.

The presented lifetimes consider only the $\cdot\text{OH}$ -oxidation reaction of an organic nitrate in both the gas- and the aqueous-phase. Further experimental data and structure activity relationships would be needed to precisely determine how hydrolysis and photolysis would affect the calculated lifetimes. However, as suggested by Reviewer 2, a better description of the calculated lifetimes for the different organic nitrate families have been included in the manuscript. Furthermore, these lifetimes have been compared in a more extensive way to the hydrolysis and photolysis lifetimes reported in the literature.

Herein are the changes done in the manuscript on line 530: "Their $\tau_{\text{OH,multiphase}}$ is dependent on the chemical structure of the molecules. Large molecules, such as terpene nitrates, or compounds with reactive groups such as aldehyde nitrates show low $\cdot\text{OH}$ -oxidation lifetimes (from 6 to 27 hours). For most of the other organic nitrates, their lifetimes range from 1 day to 1 week, such as primary alkyl nitrates, hydroxy nitrates, ketonitrates with more than 3 carbon atoms or organic nitrates containing more than one different functional group. The last category contains 4 important isoprene-derived nitrates for which multiphase $\cdot\text{OH}$ -oxidation lifetimes are 1 day for C₅ dihydroxy dinitrate, 1 day for methacrolein nitrate and 2 and 4 days for the two isomeric forms of methylvinyl nitrate. The most persistent molecules towards $\cdot\text{OH}$ present are small (≤ 3 carbon atoms), bear reactivity inhibiting functional groups such as carboxylic groups or combine more than one nitrate group. The multiphase $\cdot\text{OH}$ -oxidation lifetimes for these molecules can reach 28 days. Isopropyl nitrate and α -nitrooxyacetone, compounds which have been widely detected in the atmosphere, present very low atmospheric reactivity towards $\cdot\text{OH}$ radicals (24 and 19 days, respectively).

Among the selected organic nitrates, some compounds bear their nitrate group on a tertiary carbon; these species may undergo very fast hydrolysis (Darer et al., 2011; Jacobs et al., 2014). Their lifetimes with respect to hydrolysis range from 1 min to 8.8 h (Takeuchi and Ng, 2019). Therefore, for most of these compounds their hydrolysis is likely the main loss reaction in the atmosphere. Nevertheless, as mentioned in Section 1, the non-hydrolyzable fraction of organic nitrates ranges from 68 to 91 % for α -pinene and β -pinene derived organic nitrates thus for most of these organic nitrates this reaction does not occur.

Photolysis is also a likely sink for organic nitrates, mostly for carbonyl nitrates. Gas-phase photolysis lifetimes have been experimentally determined or simulated for eleven of these compounds and they range from 0.5 to 15 h (Barnes et al., 1993; Müller et al., 2014; Picquet-Varrault et al., 2020; Suarez-Bertoá et al., 2012). At these rates, gas-phase photolysis is expected to be the main chemical loss process for low molecular-weight carbonyl nitrates. On the other hand, to our knowledge, no aqueous-phase photolysis lifetimes have been experimentally determined for carbonyl nitrates. Meanwhile, Romonosky et al. (2015) investigated molar absorptivity of a series of β -hydroxynitrates in the aqueous-phase, and, assuming similar quantum yields as in the gas-phase, they calculated the photolysis rate constant ratios between the gas- and aqueous-phase. Using their approach, aqueous phase photolysis is likely a major sink for water soluble carbonyl nitrates as it likely occurs for most isoprene-derived nitrates. However, their results show that $\cdot\text{OH}$ -oxidation in the aqueous- or the gas-phase is a more

significant loss process than photolysis for β -hydroxynitrates. This could be the case for atmospherically relevant species such as C₅ dihydroxy dinitrate or for terpene nitrates. For the latter, their \cdot OH-oxidation lifetimes fall in the same range as the photolysis lifetimes reported for carbonyl nitrates in the gas-phase thus both processes may be relevant for terpene nitrates including those containing carbonyl groups, but further experimental studies would deserve attention to confirm this.”

(b) The aqueous (and thus multiphase) lifetimes depend on the aqueous OH concentrations. The aqueous [OH] used in the manuscript (1E-14 M) is from a numerical model and is approximately 2 – 10 times higher than measurements. For example, Kaur et al. (2018) report aqueous [OH] of approximately 5E-15M in cloud drops and an extrapolated 1E-15 M in particle water. These model-measured differences, and their impact on calculated multiphase lifetimes, should be discussed.

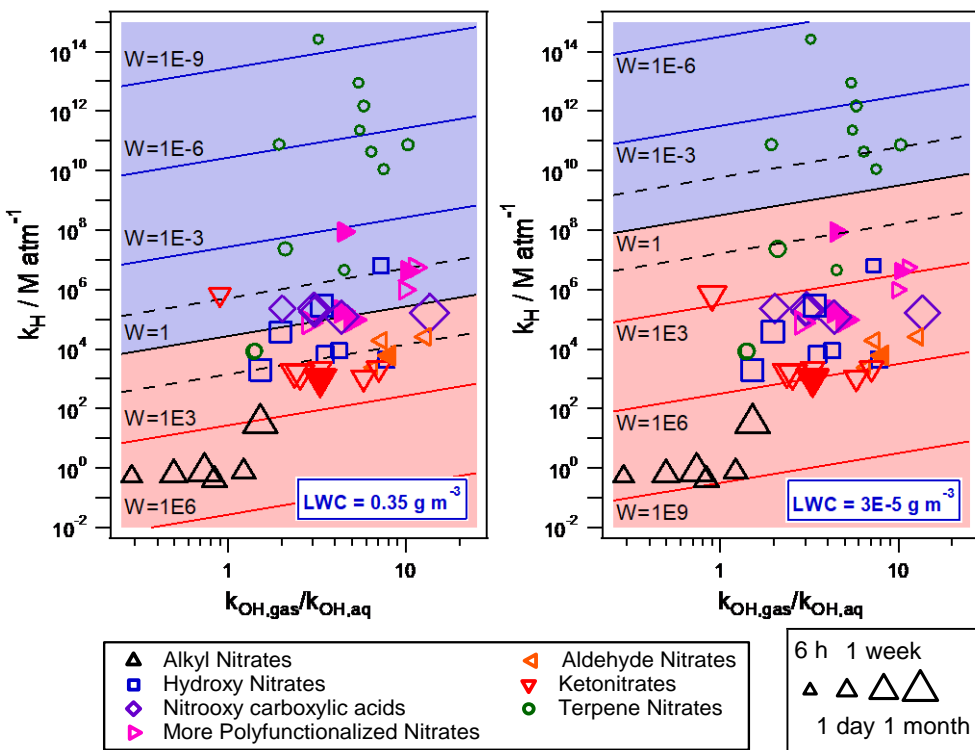
The \cdot OH radical concentration used ($1 \cdot 10^{-14}$ M) corresponds to the lowest modeled concentration value. Measured values reported by Kaur and Anastasio, (2017) correspond to \cdot OH concentrations in remote cloud droplets in winter. These concentrations are essentially extremely variable, and the value we used could match to those reported for cloud droplets in summer (Figure 1 in Arakaki et al., (2013)) or to those in cloud droplet in polluted areas. However, the possibility for lower $[\cdot\text{OH}]_{\text{aq}}$ has been discussed and included in the manuscript.

Herein are the changes done in the manuscript, in line 574: “This effect might be enhanced considering that aqueous \cdot OH concentrations might be lower than the one used in Eq. (14), i.e.: $1 \cdot 10^{-14}$ M. This value corresponds to aqueous concentrations of \cdot OH in a polluted/urban cloud droplet (Tilgner et al., 2013). Nevertheless, for remote cloud droplets or wet aerosols, the aqueous \cdot OH concentration might be 2 to 10 times lower (Arakaki et al., 2013). These lower concentrations would induce an increase of the \cdot OH-oxidation lifetimes of molecules partitioning into the aqueous-phase.”

(c) On first read, Figure 8 suggests that compounds with high W values (i.e., where most oxidation occurs in the aqueous phase) will have shorter lifetimes because of this aqueous sink. But this is not the case - for many of the compounds there is very little difference between gas-phase lifetime and multiphase (i.e., gas and PM) lifetime, as discussed only later with Figure 9. It would be helpful to incorporate the lifetimes into Figure 8, e.g., as symbol color or size, to more clearly show this. Showing the lifetimes in a figure would be very helpful, as this information is currently buried in Supplemental Table S5.

As indicated in the manuscript, a W value lower than 1 implies that more than 50% of the target compound is consumed in the aqueous-phase. Therefore, a value higher than 1 means that the gas-phase \cdot OH-oxidation reaction is more significant than the aqueous-phase reaction. The W value does not give information on the multiphase lifetime, but a compound with a low W value (where most oxidation occurs in the aqueous-phase) will tend to have a longer lifetime when considering its reaction in both phases than in the gas-phase only. This is mostly due to the lower reactivity of the nitrate group towards \cdot OH in the aqueous-phase. The compounds presenting a small difference between gas-phase lifetime and multiphase lifetime are those that barely partition to the aqueous-phase.

Figure 8 incorporating the multiphase \cdot OH-oxidation lifetimes as a function in time would look as it follows (the marker size increases proportionally to the logarithm of the lifetime):



We have not decided to include the lifetimes in Figure 8 because it increases the complexity of the figure (already with 5 dimensions). Nevertheless, as exposed above, the multiphase lifetimes were more detailed for the different organic nitrate families focusing on the chemical properties which have an influence on the lifetime. We think that this is more appropriated than including the lifetimes as a marker size.

»Other points«

Line 39. Hydrolysis to form nitrate is also an important sink for some nitrates, especially some isoprene-derived organic nitrates. Photolysis should be mentioned also.

The sentence was rearranged to also specify processes where NO_x are removed from the atmosphere. During their long-range transport, these compounds may: 1) release back NO_x far from NO_x sources via direct photolysis and/or $\cdot\text{OH}$ -oxidation or 2) act as a definitive sink of atmospheric NO_x by hydrolysis of the nitrate group and/or by deposition.

I. 79. The absolute uncertainty on the $k(\text{OH}+\text{SCN}^-)$ rate constant might be larger than the target rate constant, but this doesn't matter: it is the relative – not absolute – uncertainty (i.e., 0.20/1.12) that is propagated in the relative rate calculation to determine the uncertainty on the target compound.

We agree on this point. The sentence was removed.

I. 125. To avoid any confusion that $k(\text{OH},\text{X})$ is a pseudo-first order rate constant for loss of X , the authors should explicitly state that this is the second-order rate constant and give the units ($\text{M}^{-1} \text{s}^{-1}$).

This has been clarified.

I. 135. The method works as long as the reference and target compounds are in Henry's law equilibrium in the reaction flask. For highly reactive compounds this condition might break

down. Based on an estimated characteristic time for aqueous mixing in the flask, is there an upper limit to the rate constants that can be determined under their [OH] conditions?

There should not be any upper limit to determine high-rate constants because the developed method has the advantage to be very versatile: the reaction can be slowed down by both lowering the Fe^{2+} or adding the solution at slower speed. The reaction is produced by adding a solution of Fe^{2+} to the reactor using an automatic syringe which adds the solution continuously. By slowing the speed of the syringe, and using lower concentrations of Fe^{2+} , a highly reactive compound would be consumed in a slower way. By optimizing these parameters and with an appropriate reference compound, we expect that any molecule soluble enough can be studied using this method.

I. 243. Where is the “...previous calculation of the quantity of OH radicals...” that is referenced here?

This was an error.

We removed the sentence from the manuscript, and we have added the following one: “the ratios $k_{OH,X}/k_{OH,M}$ observed are significantly different from the gas-phase rate constant ratios, which are about 2 or 3 times higher.”

Section 3.2 Indicate how uncertainties were determined. Were they based on the standard deviation between replicates propagated with the uncertainty in the MeOH rate constant?

Yes. This has been included in the manuscript: “Uncertainties were calculated by propagating the standard deviation of the replicates with the uncertainty of the methanol k_{OH} rate constant. Then, to account for the small number of experiments performed for some molecules, the uncertainties are given by the confidence limits of 95 % given by the Student’s t-distribution.”

I. 429 (and throughout). Typically, the liquid water content abbreviation “LWC” has no subscripted portion.

L_{WC} has been changed to LWC through the whole manuscript except for Equations 11 and 13 where L_{WC} was kept for clarity in the equations.

I. 461. The gas-phase units are shown here but not described until later. Since they’re not standard, clarify here that [OH](gas) is in mol-OH / L-air and that the same volume unit is used for gas-phase rate constants.

This has been clarified.

I. 471. Both values of what?

The simulated $k_{OH,gas}$ and K_H . It has been clarified in the manuscript.

Table 2. Include the number of experiments for each compound in the table. Also indicate in the table that uncertainties are 95% CI.

This was included.

Figure 5 is a helpful comparison of data across compounds and phases.

Figure 8. Put the symbol for the isoprene-derived nitrates in the figure legend (along with the rest of the classes) rather than as a sentence in the caption.

Since there are isoprene-derived nitrates in three different families (aldehydes, keto and with more than 2 different functions) we should incorporate three different symbols or create a new different one. We believe it is easier to specify that filled symbols correspond to an isoprene-derived nitrate and keeping the information related to their functionalization.

Figure 9. Include another panel that shows the analogous results for the cloud LWC condition.

Figure 9 already include cloud LWC content conditions. However, we have added another panel with wet aerosol LWC conditions.

A discussion over Figure 9b has been included in the manuscript in line 579: “Figure 9b shows that under wet aerosol conditions, only terpene nitrates ·OH-oxidation lifetimes are affected when considering the aqueous-phase. Under this LWC condition, the proposed terpene nitrates partition both in the aqueous- and the aerosol-phase (Figure 7b). In the aerosol-phase, not only the ·OH-oxidation kinetic rate constants may differ from the gas- and the aqueous-phase ones but also other oxidants can play a crucial role in the atmospheric loss of these compounds (Kaur and Anastasio, 2018; Manfrin et al., 2019). Further studies comprising this reactivity are thus needed to better understand the fate of organic nitrates in all atmospheric phases.”

The SI does not have a list of references.

A bibliography section was added.

Table S5 includes the multiphase lifetime for the particle LWC condition, but not for the cloud LWC condition. The latter should be included.

Table S5 includes cloud LWC condition multiphase lifetime and gas-phase lifetime (no LWC). However, since Figure 9b shows that for most of the proposed organic nitrates their multiphase lifetime under wet aerosol conditions barely differs from the gas-phase lifetimes except for terpene nitrates. Therefore, we only have included the lifetime under particle LWC conditions for the latest compounds.

References

Arakaki, T., Anastasio, C., Kuroki, Y., Nakajima, H., Okada, K., Kotani, Y., Handa, D., Azechi, S., Kimura, T., Tsuhako, A. and Miyagi, Y.: A General Scavenging Rate Constant for Reaction of Hydroxyl Radical with Organic Carbon in Atmospheric Waters, , doi:10.1021/es401927b, 2013.

Ashton, L., Buxton, G. V and Stuart, C. R.: Temperature dependence of the rate of reaction of OH with some aromatic compounds in aqueous solution. Evidence for the formation of a π -complex intermediate?, J. Chem. Soc. Faraday Trans., 91(11), 1631–1633, 1995.

Barnes, I., Becker, K. H. and Zhu, T.: Near UV absorption spectra and photolysis products of difunctional organic nitrates: Possible importance as NO_x reservoirs, J. Atmos. Chem., 17(4), 353–373, doi:10.1007/BF00696854, 1993.

Buxton, G. V, Greenstock, C. L., Helman, W. P. and Ross, A. B.: Critical Review of rate constants for reactions of hydrated electrons, hydrogen atoms and hydroxyl radicals (?OH/?O ? in Aqueous Solution, J. Phys. Chem. Ref. Data, 17(2), 513–886, doi:10.1063/1.555805, 1988.

Darer, A. I., Cole-Filipliak, N. C., Connor, A. E. O. and Elrod, M. J.: Formation and Stability of Atmospherically Relevant Isoprene-Derived Organosulfates and Organonitrates, Environ. Sci. Technol., 45, 1895–1902, 2011.

Doussin, J.-F. and Monod, A.: Structure–activity relationship for the estimation of OH-oxidation rate constants of carbonyl compounds in the aqueous phase, Atmos. Chem. Phys., 13(23), 11625–11641, doi:10.5194/acp-13-11625-2013, 2013.

Heath, A. A. and Valsaraj, K. T.: Effects of Temperature, Oxygen Level, Ionic Strength, and pH on the Reaction of Benzene with Hydroxyl Radicals at the Air-Water Interface in Comparison to the Bulk Aqueous Phase, J. Phys. Chem. A, 119(31), 8527–8536, doi:10.1021/acs.jpca.5b05152, 2015.

Herrmann, H., Hoffmann, D., Schaefer, T., Bräuer, P. and Tilgner, A.: Tropospheric aqueous-phase free-radical chemistry: Radical sources, spectra, reaction kinetics and prediction tools, ChemPhysChem, 11(18), 3796–3822, doi:10.1002/cphc.201000533, 2010.

Jacobs, M. I., Burke, W. J. and Elrod, M. J.: Kinetics of the reactions of isoprene-derived hydroxynitrates: gas phase epoxide formation and solution phase hydrolysis, *Atmos. Chem. Phys.*, 14(17), 8933–8946, doi:10.5194/acp-14-8933-2014, 2014.

Kaur, R. and Anastasio, C.: Light absorption and the photoformation of hydroxyl radical and singlet oxygen in fog waters, *Atmos. Environ.*, 164, 387–397, doi:10.1016/j.atmosenv.2017.06.006, 2017.

Kroflič, A., Schaefer, T., Huš, M., Phuoc Le, H., Otto, T. and Herrmann, H.: OH radicals reactivity towards phenol-related pollutants in water: Temperature dependence of the rate constants and novel insights into the [OH-phenol] adduct formation, *Phys. Chem. Chem. Phys.*, 22(3), 1324–1332, doi:10.1039/c9cp05533a, 2020.

Land, E. J. and Ebert, M.: Pulse radiolysis studies of aqueous phenol. Water elimination from dihydroxycyclohexadienyl radicals to form phenoxy., 1967.

Monod, A. and Doussin, J. F.: Structure-activity relationship for the estimation of OH-oxidation rate constants of aliphatic organic compounds in the aqueous phase: alkanes, alcohols, organic acids and bases, *Atmos. Environ.*, 42(33), 7611–7622, doi:10.1016/j.atmosenv.2008.06.005, 2008.

Müller, J. F., Peeters, J. and Stavrakou, T.: Fast photolysis of carbonyl nitrates from isoprene, *Atmos. Chem. Phys.*, 14(5), 2497–2508, doi:10.5194/acp-14-2497-2014, 2014.

Neyens, E. and Baeyens, J.: A review of classic Fenton's peroxidation as an advanced oxidation technique, *J. Hazard. Mater.*, 98(1–3), 33–50, doi:10.1016/S0304-3894(02)00282-0, 2003.

Peduzzi, P., Concato, J., Kemper, E., Holford, T. R. and Feinstein, A. R.: A simulation study of the number of events per variable in logistic regression analysis, *J. Clin. Epidemiol.*, 49(12), 1373–1379, doi:10.1016/S0895-4356(96)00236-3, 1996.

Picquet-Varraud, B., Suarez-Bertoa, R., Duncianu, M., Cazaunau, M., Pangui, E., David, M. and Doussin, J.-F.: Photolysis and oxidation by OH radicals of two carbonyl nitrates: 4-nitrooxy-2-butanone and 5-nitrooxy-2-pentanone, *Atmos. Chem. Phys.*, 20(1), 487–498, doi:10.5194/acp-20-487-2020, 2020.

Rindelaub, J. D., Borca, C. H., Hostetler, M. A., Slade, J. H., Lipton, M. A., Slipchenko, L. V. and Shepson, P. B.: The acid-catalyzed hydrolysis of an α -pinene-derived organic nitrate: kinetics, products, reaction mechanisms, and atmospheric impact, *Atmos. Chem. Phys.*, 16(23), 15425–15432, doi:10.5194/acp-16-15425-2016, 2016.

Smith, J. D., Kinney, H. and Anastasio, C.: Aqueous benzene-diols react with an organic triplet excited state and hydroxyl radical to form secondary organic aerosol, *Phys. Chem. Chem. Phys.*, 17(15), 10227–10237, doi:10.1039/c4cp06095d, 2015.

Suarez-Bertoa, R., Picquet-Varraud, B., Tamas, W., Pangui, E. and Doussin, J. F.: Atmospheric fate of a series of carbonyl nitrates: Photolysis frequencies and OH-oxidation rate constants, *Environ. Sci. Technol.*, 46(22), 12502–12509, doi:10.1021/es302613x, 2012.

Takeuchi, M. and Ng, N. L.: Chemical composition and hydrolysis of organic nitrate aerosol formed from hydroxyl and nitrate radical oxidation of α -pinene and β -pinene, *Atmos. Chem. Phys.*, 19, 12749–12766, doi:10.5194/acp-19-12749-2019, 2019.

Tilgner, A., Bräuer, P., Wolke, R. and Herrmann, H.: Modelling multiphase chemistry in deliquescent aerosols and clouds using CAPRAM3.0i, *J. Atmos. Chem.*, 70(3), 221–256, doi:10.1007/s10874-013-9267-4, 2013.

On the importance of atmospheric loss of organic nitrates by aqueous-phase ·OH-oxidation

Juan Miguel González-Sánchez^{1,2}, Nicolas Brun^{1,2}, Junteng Wu¹, Julien Morin¹, Brice Temime-Rousell¹, Sylvain Ravier¹, Camille Mouchel-Vallon³, Jean-Louis Clément², Anne Monod¹

5 ¹ Aix Marseille Univ, CNRS, LCE, Marseille, France

² Aix Marseille Univ, CNRS, ICR, Marseille, France

³ Laboratoire d'Aérologie, Université de Toulouse, CNRS, UPS, Toulouse, France

Correspondence to: Juan Miguel González-Sánchez (juanmiguelgs93@gmail.com) and Anne Monod (anne.monod@univamu.fr)

10 **Abstract.** Organic nitrates are secondary species in the atmosphere. Their fate is related to the chemical transport of pollutants from polluted areas to more distant zones. While their gas-phase chemistry has been studied, their reactivity in condensed phases is far from being understood. However, these compounds represent an important fraction of organic matter in condensed phases. In particular, their partition to the aqueous-phase may be especially important for oxidized organic nitrates for which water solubility increases with functionalization. This work has studied for the first time the aqueous-phase ·OH-oxidation
15 kinetics of 4 alkyl nitrates (isopropyl nitrate, isobutyl nitrate, 1-pentyl nitrate **and isopentyl nitrate**) and 3 functionalized organic nitrates (α -nitrooxyacetone, 1-nitrooxy-2-propanol and isosorbide 5-mononitrate) by developing a novel and accurate competition kinetic method. Low reactivity was observed, with k_{OH} ranging from $8 \cdot 10^7$ to $3.1 \cdot 10^9 \text{ L mol}^{-1} \text{ s}^{-1}$ at $296 \pm 2 \text{ K}$. Using these results, a previously developed aqueous-phase Structure Activity Relationship (SAR) was extended, and the resulting parameters confirmed the extreme deactivating effect of the nitrate group, up to two adjacent carbon atoms. The
20 achieved extended SAR was then used to determine the ·OH-oxidation rate constants of 49 organic nitrates, including hydroxy nitrates, ketonitrates, aldehyde nitrates, nitrooxy carboxylic acids and more functionalized organic nitrates such as isoprene and terpene nitrates. Their multiphase atmospheric lifetimes towards ·OH-oxidation were calculated using these rate constants and they were compared to their gas-phase lifetimes. Large differences were observed, especially for polyfunctional organic nitrates: for 50% of the proposed organic nitrates for which ·OH-reaction occurs mainly in the aqueous-phase (more than 50%
25 of the overall removal) their ·OH-oxidation lifetimes increased by 20% to 155% under cloud/fog conditions ($\text{LWC} = 0.35 \text{ g m}^{-3}$). In particular, for 83% of the proposed terpene nitrates, the reactivity towards ·OH occurred mostly ($> 98\%$) in the aqueous-phase while for 60% of these terpene nitrates their lifetimes increased by 25% to 140% compared to their gas-phase reactivity. We demonstrate that these effects are of importance under cloud/fog conditions, but also under wet aerosol conditions, especially for the terpene nitrates. These results suggest that considering aqueous-phase ·OH-oxidation reactivity
30 of biogenic nitrates is necessary to improve the predictions of their atmospheric fate.

1 Introduction

Nitrogen oxides ($\text{NO}_x = \cdot\text{NO} + \cdot\text{NO}_2$) intensely impact air quality and the environment as they play key roles in the production of relevant air pollutants such as ozone (O_3), nitrous acid (HONO), nitric acid (HNO_3) and secondary organic aerosol (SOA). Their atmospheric chemistry controls the concentrations of the three main oxidants, O_3 , $\cdot\text{OH}$ and $\text{NO}_3\cdot$ radicals. The past few

35 decades have witnessed important reduction in NO_x direct emissions in Europe or North America resulting in changes in their atmospheric fate, by increasing the relative importance of their conversion to organic nitrates (Romer Present et al., 2020).

The latter are secondary organic compounds, formed by the reactivity of NO_x with volatile organic compounds (VOCs). Owing to their long atmospheric lifetimes (much longer than for NO_x), organic nitrates can be transported from polluted to remote areas.

36 During their long-range transport, these compounds may: 1) release back NO_x far from NO_x sources via direct photolysis and/or $\cdot\text{OH}$ -oxidation or 2) act as a definitive sink of atmospheric NO_x by hydrolysis of the nitrate group and/or by deposition.

40 Organic nitrates thus act as sinks and reservoirs of NO_x , leading to a broader spatial distribution of NO_x and thus spreading the ozone, HONO and SOA formation from the local to the regional scale. For this reason, understanding and considering the reactivity of organic nitrates is necessary for accurately predicting their atmospheric fates and impacts on air quality.

45 The gas-phase chemistry of organic nitrates has been studied through kinetic experiments focusing on their $\cdot\text{OH}$ -oxidation (Bedjanian et al., 2018; Picquet-Varraud et al., 2020; Treves and Rudich, 2003; Wängberg et al., 1996; Zhu et al., 1991) and

46 direct photolysis (Clemitschaw et al., 1997; Picquet-Varraud et al., 2020; Suarez-Bertoa et al., 2012). These experiments provide data for different types of organic nitrates, including alkyl nitrates, ketonitrates, hydroxy nitrates, dinitrates, cyclonitrates and alkene nitrates, and provide knowledge on their gas-phase atmospheric fate. Although alkyl and alkene

50 nitrates are highly volatile, polyfunctional organic nitrates may show much lower volatility and they can partition to condensed phases as aqueous- and aerosol-phase. Their presence in submicron particles has been observed in a fraction ranging from 5 to 77 % (in mass) of organic aerosol in Europe and North America (Kiendler-Scharr et al., 2016; Lee et al., 2019). Despite this fact, their reactivities in condensed phases were poorly explored. Most studies have focused on hydrolysis, a reaction that is extremely structure dependent, mostly occurring to tertiary or allylic nitrates (Hu et al., 2011; Liu et al., 2012), while the non-hydrolyzable fraction of α - and β -pinene particulate organic nitrate ranges from 68 to 91 % in mass (Takeuchi and Ng, 2019).

55 To our knowledge, only one study experimentally determined the photolysis kinetics of organic nitrates in the aqueous-phase (Romonosky et al., 2015) and concluded that the $\cdot\text{OH}$ removal processes should have a higher relevance. However, there has been no attempts to experimentally determine their aqueous-phase $\cdot\text{OH}$ -oxidation reactivity.

60 Aqueous-phase $\cdot\text{OH}$ -oxidation processes play a key role in the removal and the production of water soluble compounds in the atmosphere (Herrmann et al., 2015). The determination of kinetic rate constants is essential to understand their lifetimes and

65 to develop more precise models to predict pollution events and the scale of pollutants' transportation. Determining aqueous-phase $\cdot\text{OH}$ -oxidation second order rate constants (k_{OH}) may be done by a direct method, measuring $\cdot\text{OH}$ concentrations in the aqueous phase by UV-VIS absorption, with however troublesome interferences of absorbance of organic molecules within the same wavelength region (Herrmann et al., 2010). competition kinetic methods have been then widely developed. These

65 methods consist ~~eonsisting~~ in the comparison between the decay of the target compound versus a reference compound, for which k_{OH} value is well-known. Many studies have used the thiocyanate anion (SCN^-) as the reference compound. Its decay can be easily followed by online spectroscopic measurement of the formed radical anion (SCN_2^-) in presence and in absence of the target compound (Herrmann, 2003). This technique, however, is not well suited for low reactive species for which $k_{OH} \leq 10^9 L mol^{-1} s^{-1}$, i.e., more than 10 times lower than $k_{OH + SCN} = 1.12 (\pm 0.20) \cdot 10^{10} L mol^{-1} s^{-1}$. In this case, the target species should reach high concentrations to be able to compete with the thiocyanate anion. These high concentrations may interfere 70 with the measurements. ~~Furthermore, the uncertainty on $k_{OH + SCN}$ may be higher than the target compound rate constant.~~ Other indirect methods use offline measurements for monitoring the target and reference compounds. However, most of these methods use reference compounds for which k_{OH} values have not been so widely explored thus inducing important uncertainties to the experimentally determined k_{OH} values (Herrmann, 2003).

75 The aim of this work was to accurately determine aqueous-phase k_{OH} rate constants by developing a new online competition kinetic method, well suited to low reactivity species. The effectiveness and the relevance of the method were validated on compounds for which k_{OH} rate constants are well-known. Then, the method was used to determine the k_{OH} rate constants of some organic nitrates and the results were used to extend the aqueous-phase Structure Activity Relationship (SAR) developed earlier (Monod and Doussin, 2008 and Doussin and Monod, 2013) to the nitrate group. Furthermore, the prediction of k_{OH} rate constants for other atmospherically relevant organic nitrates in the aqueous-phase was performed with the extended SAR.

80 Finally, the potential multiphase fate in the atmosphere of these compounds was estimated.

2 Experimental

2.1 Principle

85 The originality of this work relies on a competition kinetic method monitored by online decay measurements of the reference compound in the reactor's headspace using a Proton Transfer Reaction-Mass Spectrometer (PTR-MS). Concerning the target compounds, depending on their properties (solubility, volatility, and instrumental response), their kinetic decays were monitored in the reactor's headspace by PTR-MS or off-line by Ultra-High-Performance Liquid Chromatography-Photodiode Array detector (UHPLC-UV). The developed method employed methanol as the reference compound because: i) its k_{OH} rate constant, $9.7 (\pm 1.5) \cdot 10^8 L mol^{-1} s^{-1}$ at 298 K, is widely accepted (Table S1); ii) this value is relevant for competitive kinetics relative to low reactive species, and iii) its extremely sensitive quantification by PTR-MS was expected to not suffer from any 90 interferences with the selected organic nitrates (Aoki et al., 2007; Lindinger et al., 1998).

Due to the known sensitivity of organic nitrates to photolysis (Romonosky et al., 2015), aqueous $\cdot OH$ radicals were generated in the dark by the Fenton reaction (R1) (Neyens and Baeyens, 2003) by dropwise addition of a solution of Fe^{2+} to an acidic solution of H_2O_2 in excess containing methanol and the target compound.



95 The method was validated using isopropanol and acetone as target compounds, whose ·OH-oxidation rate constants are well-known (Table S1). The method was then used to determine new k_{OH} values for four alkyl nitrates (isopropyl nitrate, isobutyl nitrate, 1-pentyl nitrate **and** isopentyl nitrate **and** 2-ethylhexyl nitrate) and three polyfunctional organic nitrates (α -nitrooxyacetone, 1-nitrooxy-2-propanol and isosorbide 5-mononitrate), see Table 1. Furthermore, a tentative study of 2-ethylhexyl nitrate k_{OH} rate constant was performed using this method, but it was limited by its very low solubility.

100 **2.2 Experimental setup and protocol**

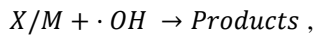
The aqueous-phase reactor consisted in a one-liter three-neck round-bottom flask closed hermetically with rubber caps (Fig. 1). A Razel syringe pump at 0.33 mL min^{-1} was used with a glass syringe to add dropwise a solution of Fe^{2+} into the reactor's aqueous solution. A second syringe was also connected to the reactor to add the target and the reference compound and to sample the aqueous-phase when necessary. The aqueous reactor's solution was continuously stirred before and during the 105 reaction with a magnetic stirrer. A flow of synthetic air constantly guided a fraction of the headspace gas-phase of the reactor to the PTR-MS instrument, with a flow of 0.050 L min^{-1} using a mass flow controller (Brooks SLA Series). A 1:30 dilution was performed downward the reactor's flow using synthetic air at 1.450 L min^{-1} . All experiments were performed at room temperature ($296 \pm 2 \text{ K}$).

In each experiment, the Fe^{2+} solution consisted in $5 - 10 \text{ mL}$ of $\text{FeSO}_4 \cdot 7\text{H}_2\text{O}$ ($0.02 - 0.06 \text{ mol L}^{-1}$), added dropwise to the 110 solution of 400 mL of H_2O_2 (in excess, i.e., 0.004 mol L^{-1}) acidified by H_2SO_4 (0.005 mol L^{-1}), to keep **pH = 2.5 (Micro pH electrode, Thermo)** during the reaction. Concentrations and volumes of the Fe^{2+} solution were varied in order to optimize the ·OH attack to the reference and the target compound. All experiments and their initial conditions are compiled on Table S2. The Fe^{2+} solution was used as the limiting reagent to minimize its possible interferences with the organic nitrate reaction products. In addition, it was verified in control experiments that H_2O_2 , used in excess, did not react with any of the target 115 compounds. **Furthermore, control experiments at pH = 2.5 confirmed that none of the organic nitrates underwent hydrolysis at significant rates under our experimental conditions.**

Prior to each experiment, the reactor's headspace was extensively purged with pure air for 1 hour while PTR-MS measurements were set for stabilization purposes. The target compound and methanol were then added directly into the aqueous-phase and the reactor's headspace signal was monitored for 30 minutes before the reaction with constant stirring of the solution to 120 determine the first order rate constant of evaporation (k_{vap}) of each compound under the reaction conditions. The reaction was then started by adding dropwise the Fe^{2+} solution for 15 to 30 minutes (depending on the volume of Fe^{2+} added). During experiments performed with isopropyl nitrate, α -nitrooxyacetone, 1-nitrooxy-2-propanol and isosorbide 5-mononitrate, the aqueous-phase was sampled every three minutes for off-line measurements by UHPLC-UV. Once the flow of Fe^{2+} was stopped, the system was kept stirring for another 30 minutes while continuously monitoring the reactor's headspace.

125 **2.3 Methodology**

In such a competition between the target compound (X) and methanol (M) towards ·OH radicals (R2),



(R2)

in the absence of direct photolysis, the second-order kinetic rate constant of the target compound, $k_{OH,X}$ (in $L \text{ mol}^{-1} \text{ s}^{-1}$), is directly obtained from the slope ($k_{OH,X}/k_{OH,M}$) of the linear plot of $\ln ([X]_0 \text{ (aq)}/[X]_t \text{ (aq)})$ versus $\ln ([M]_0 \text{ (aq)}/[M]_t \text{ (aq)})$ derived from Eq. (1).

$$\ln \frac{[X]_0 \text{ (aq)}}{[X]_t \text{ (aq)}} = \frac{k_{OH,X}}{k_{OH,M}} \cdot \ln \frac{[M]_0 \text{ (aq)}}{[M]_t \text{ (aq)}}, \quad (1)$$

where $([X]_0 \text{ (aq)}/[X]_t \text{ (aq)})$ represents the aqueous-phase concentration relative decay of the target compound, and $([M]_0 \text{ (aq)}/[M]_t \text{ (aq)})$ the aqueous-phase concentration relative decay of methanol.

Using the Fenton reaction (R1), $\cdot OH$ radicals were generated within the aqueous-phase and could not reach the headspace in sufficient amounts to react significantly with the target compounds in the gas-phase. This was confirmed by the validation experiments (section 3.1) where the values found for $k_{OH,X}/k_{OH,M}$ ratios were those of the aqueous-phase reactions, and not those of the gas-phase which are a factor of 2 to 3 higher.

Headspace analyses were based on the direct proportionality between aqueous- and gas-phase concentrations of the analytes (Karl et al., 2003). Therefore, in cases where both the target and the reference compounds were monitored by PTR-MS, Eq. (1) can be written as Eq. (2), (see Appendix A for detailed explanations),

$$\ln \frac{ncps(X)_0}{ncps(X)_t} = \frac{k_{OH,X}}{k_{OH,M}} \cdot \ln \frac{ncps(M)_0}{ncps(M)_t}, \quad (2)$$

where $ncps(X)$ and $ncps(M)$ are the normalized count rate of respectively the target compound and methanol, i.e.: $ncps(X) = \sum cps(X^+)/cps(H_3O^+)$ and $ncps(M) = \sum cps(M^+)/cps(H_3O^+)$. The normalization to the H_3O^+ count rate removes any signal variability due to fluctuating performances of the ion source.

Depending on the properties of the investigated organic nitrates (i.e., their water solubility, volatility, and instrumental response), different treatments were applied to determine their kinetic decays. All the very volatile compounds were monitored in the reactor's headspace by PTR-MS: this comprised the target alkyl nitrates (for which Henry's Law constant $K_H < 1 \text{ mol L}^{-1} \text{ atm}^{-1}$), as well as methanol, acetone, and isopropanol ($K_H < 300 \text{ mol L}^{-1} \text{ atm}^{-1}$). Furthermore, due to the low water solubility of alkyl nitrates, their initial concentrations were limited to $5 \cdot 10^{-5} \text{ mol L}^{-1}$. On the other hand, the target polyfunctionalized organic nitrates were much less volatile ($K_H > 1000 \text{ mol L}^{-1} \text{ atm}^{-1}$) and their detection by PTR-MS was more problematic, their relative decays were monitored in the aqueous-phase by off-line UHPLC-UV. For these compounds, the determination of the aqueous-phase $\cdot OH$ -oxidation rate constant was performed by plotting the relative decay of the aqueous-phase concentration ($\ln ([X]_0 \text{ (aq)}/[X]_t \text{ (aq)})$) against the relative decay of the reference compound signal in the gas-phase ($\ln (ncps(M)_0/ncps(M)_t)$) as shown in Eq. (3):

$$\ln \frac{[X]_0 \text{ (aq)}}{[X]_t \text{ (aq)}} = \frac{k_{OH,X}}{k_{OH,M}} \cdot \ln \frac{ncps(M)_0}{ncps(M)_t}, \quad (3)$$

In addition, for the most volatile molecules (i.e., alkyl nitrates), further corrections were performed to subtract the contribution of evaporation to the overall reaction decay. Their high volatilities induced a substantial decay of their concentrations that was systematically measured prior to the start of the reaction, inferring a specific first order rate constant of evaporation (k_{vap}) of each compound under the reaction conditions. While for methanol, acetone, or isopropanol the evaporation decay was negligible, for the alkyl nitrates it accounted for 2 to 20% of the molecule's consumption during the reaction. To consider this contribution, Eq. (4) was used instead of Eq. (2) for volatile alkyl nitrates:

$$\frac{1}{t} \cdot \ln \frac{ncps(X)_0}{ncps(X)_t} = k_{vap} + \frac{k_{OH,X}}{k_{OH,M}} \cdot \frac{1}{t} \cdot \ln \frac{ncps(M)_0}{ncps(M)_t}, \quad (4)$$

where t is the reaction time (in seconds). Plotting $1/t \cdot \ln (ncps(X)_0/ncps(X)_t)$ versus $1/t \cdot \ln (ncps(M)_0/ncps(M)_t)$ resulted in a straight line with a slope of $k_{OH,X}/k_{OH,M}$ and an intercept of k_{vap} . The value of k_{vap} was determined during the 160 30 minutes prior to the reaction and its value was fixed in Eq. (4). This treatment was not necessary for methanol, acetone or isopropanol, due to their lower volatilities. For isopropyl nitrate, which decay was also monitored in the aqueous-phase by UHPLC-UV, Eq. (5) was used (in addition to Eq. (4)):

$$\frac{1}{t} \cdot \ln \frac{[X]_0 (aq)}{[X]_t (aq)} = k_{vap} + \frac{k_{OH,X}}{k_{OH,M}} \cdot \frac{1}{t} \cdot \ln \frac{ncps(M)_0}{ncps(M)_t}, \quad (5)$$

In summary, the aqueous-phase \cdot OH-oxidation rate constant of isopropanol and acetone was determined using Eq. (2); while 170 Eq. (3) was used for determining the rate constants of α -nitrooxyacetone, 1-nitrooxy-2-propanol and isosorbide 5-mononitrate. For isobutyl nitrate, 1-pentyl nitrate and isopentyl nitrate and 2-ethylhexyl nitrate, compounds which undergo a significant evaporation decay, Eq. (4) was used. Finally, isopropyl nitrate was chosen for intercomparing both methods as it is water soluble and volatile enough to be monitored by both analytical techniques, its aqueous-phase k_{OH} was determined by both Eq. (4) and Eq. (5).

175 2.4 Analytical measurements

2.4.1 PTR-MS

A commercial high-sensitivity quadrupole PTR-MS (Ionicon Analytik GmbH) was used to monitor the concentration decay of the reference compound (methanol) and 7 target compounds (acetone, isopropanol, isopropyl nitrate, isobutyl nitrate, 1-pentyl nitrate, isopentyl nitrate and 2-ethylhexyl nitrate) during the reaction. The drift tube voltage was 600 V, the reactor 180 chamber pressure was 2.19 mbar and the drift tube temperature was 333 K. These values correspond to an E/N value of 136 Townsend (1 Townsend = 10^{-17} V cm $^{-2}$), where E is the electric field strength (V cm $^{-1}$) and N is the ambient air number density within the drift tube (molecule cm $^{-3}$). Measurements were performed using the Multiple Ion Detection (MID) mode on a short list of 11 – 13 preselected m/z values resulting in measurement cycles of 25 – 35 s. This list includes the hydronium ion isotope H $_3$ ¹⁸O $^+$ (m/z = 21) and its water clusters, H $_2$ O \cdot H $_3$ O $^+$ and (H $_2$ O) $_2$ \cdot H $_3$ O $^+$ (m/z = 37 and m/z = 55 respectively) as well as parasitic 185 ions NO $^+$ and O $_2$ $^+$ (m/z = 30 and m/z = 32) for diagnostic purpose. The remaining ions correspond to the protonated reference

compound, methanol ($m/z = 33$), and to the 5 – 7 major products of organic nitrates. The individual fragmentation patterns of the organic nitrates determined during a series of preliminary measurements in scan mode (21 – 200 amu) are listed in Table S3. Data were corrected by normalizing the ion signals with the number of hydronium ions in the drift tube, calculated by multiplying by 500 the signal at $m/z = 21$.

190 Isopentyl nitrate and 2-ethylhexyl nitrate were analyzed by PTR-MS for the first time. The other compounds, isopropyl nitrate, isobutyl nitrate and 1-pentyl nitrate were previously investigated by Duncianu et al., 2017 and Aoki et al., 2007. Table S3 compiles detected fragments and their relative intensities for all the studied organic nitrates in this work. Compared to the previous studies, similar trends in the fragmentation of organic nitrates were found. Fragments with the highest relative intensities correspond to the R^+ fragment, produced after the nitrate group loss in the drift tube, and to the NO_2^+ ion, which 195 was detected for all organic nitrates, except for 2-ethylhexyl nitrate. Other relevant fragments were the RO^+ fragment and/or other ions (such as $C_3H_5^+$, $C_3H_7^+$, $C_4H_9^+$) which were formed by further fragmentation of the R^+ fragment.

The minimum standard sensitivity normalized to 10^6 hydronium ions for all organic nitrates was determined prior to the start 200 of the reaction, by calculating the maximum possible gas-phase concentrations assuming the Henry's Law equilibrium (see Table S3). The sensitivities range from 3 to 7 ncps ppbv $^{-1}$ for all organic nitrates. From these sensitivities, it was calculated that in the reactor's headspace, the target organic nitrates were detectable at concentrations higher than $1 \cdot 10^{-7}$ mol L $^{-1}$ in the aqueous-phase.

For methanol, assuming Henry's Law equilibrium, using a $K_H = 204$ mol L $^{-1}$ atm $^{-1}$ (average value out of those reported in Sander, 2015), the minimum standard sensitivity normalized to 10^6 hydronium ions would be 9 ± 1 ncps ppbv $^{-1}$, corresponding to an effective sensitivity > 360 cps ppbv $^{-1}$ at the typical H_3O^+ count rate $4 \cdot 10^7$ cps. Under these conditions, it would be 205 detectable in the reactor's headspace at aqueous concentrations higher than $9 \cdot 10^{-6}$ mol L $^{-1}$.

2.4.2 UHPLC-UV

All the investigated organic nitrates show an intense UV absorption around 200 nm (Fig. S1). Aliquots of the solution were sampled every 3 minutes from the reactor and the least volatile target compounds were quantified by UHPLC-UV (Thermo 210 Scientific Accela 600) at 200 nm. The device was equipped with a Hypersil Gold C18 column (50 x 2.1 mm) with a particle size of 1.9 μ m and an injection loop of 5 μ L. A binary eluent of H_2O and CH_3CN was used for all analyses at a flow rate of 400 μ L min $^{-1}$. Two gradients were used depending on the compounds' polarity. For isopropyl nitrate, the gradient started from H_2O/CH_3CN 80/20 (v/v) to 50/50 (v/v) for 3 min, held at this proportion for 1 minute and then set back to 80/20 (v/v) within 215 10 seconds until the end of the run, at minute 5 (Method A). For more polar compounds, i.e. α -nitrooxyacetone, 1-nitrooxy-2-propanol and isosorbide 5-mononitrate, a similar gradient was employed but the initial and final proportions were H_2O/CH_3CN 90/10 (v/v) in order to optimize their retention times (Method B).

Calibration curves were optimized to obtain a good linearity between $5 \cdot 10^{-5}$ mol L $^{-1}$ and $1 \cdot 10^{-3}$ mol L $^{-1}$ with a $R^2 > 0.9995$. The retention times were 0.9, 1.1, 1.2 and 2.4 min for 1-nitrooxy-2-propanol, isosorbide 5-mononitrate, α -nitrooxyacetone and

isopropyl nitrate, respectively. Limits of detection are $9 \cdot 10^{-6}$ mol L⁻¹ for isopropyl nitrate and $1 \cdot 10^{-5}$ mol L⁻¹ for the other three compounds.

220 2.5 Reagents

225 Chemicals were commercially available and used as supplied: isopropyl nitrate (96%, Sigma Aldrich), isobutyl nitrate (98%, Sigma Aldrich), 2-ethylhexyl nitrate (97%, Sigma Aldrich), 1-pentyl nitrate (98%, TCI Chemicals), isopentyl nitrate (98%, TCI Chemicals), isosorbide 5-mononitrate (98%, Acros Organics), H₂O₂ (30%, non-stabilized, Acros Organics), FeSO₄·7H₂O (99%, Sigma Aldrich), H₂SO₄ (95-98%, Merck), chloroacetone (95%, Sigma Aldrich), AgNO₃ (99%, VWR Chemicals), KI (98%, Sigma Aldrich) and NaBH₄ (98%, Sigma Aldrich). Methanol (Fisher Chemical), acetonitrile (Fisher Optima) and isopropanol (Honeywell) were LC/MS grade and used as supplied. Acetone (Carlo Erba Reagents) and ether (Fisher Chemical) were HPLC grade. Tap water was purified with a Millipore MiliQ system (18.2 MΩ cm and TOC < 2 ppb).

230 Non-commercial organic nitrates, i.e. α -nitrooxyacetone and 1-nitrooxy-2-propanol were synthesized and purified. α -Nitrooxyacetone was synthesized by the nucleophilic substitution reaction of iodoacetone which was synthesized previously from chloroacetone. The ketone group from α -nitrooxyacetone was reduced to produce 1-nitrooxy-2-propanol. See S1 for further details.

3 Results & Discussion

3.1 Validation of the kinetic method

235 Three different kinds of validation experiments were performed. Their goals were 1) to verify that the partition of the reactants between the aqueous-phase and the gas-phase (in the reactor's headspace) was rapidly reached during the reaction; 2) to intercompare the two methods (PTR-MS and UHPLC-UV); and 3) to validate the aqueous-phase kinetic k_{OH} rate constants using well known values, i.e. those of acetone and isopropanol.

240 Figure 2a shows the headspace signal measured by PTR-MS during the aqueous-phase ·OH-oxidation of isopropyl nitrate. Light blue background indicates periods when the solution of Fe²⁺ (0.06 M) was dripped into the reactor to produce ·OH radicals. One can clearly observe how the isopropyl nitrate signal decay starts immediately at the beginning of the addition of Fe²⁺ and ceases promptly when it is stopped. The partition between the aqueous-phase and the reactor's headspace is therefore swiftly reached and is faster than the PTR-MS measurement cycle rate (25 s for the shortest cycle).

245 Figure 2b shows the isopropyl nitrate decay during its aqueous-phase ·OH-oxidation while monitoring its concentration with the PTR-MS and the UHPLC-UV. It is clear from the figure that the kinetics are identical for both methods. Furthermore, the ratios $k_{OH, isopropyl\ nitrate} / k_{OH, methanol}$ were 0.29 (± 0.06) and 0.31 (± 0.06) using respectively the PTR-MS method, Eq. (4), and the UHPLC-UV one, Eq. (5). These results obtained for isopropyl nitrate confirm that its gas-phase concentrations in the reactor's headspace are proportional to its aqueous-phase concentrations. In addition, this proves that there is no ·OH attack

in the gas-phase: the ratios $k_{OH,X}/k_{OH,M}$ observed are significantly different from the gas-phase rate constant ratios, which are about 2 or 3 times higher. with our previous calculation of the quantity of $\cdot\text{OH}$ radicals that partitions to the reactor's headspace.

250 Furthermore, it shows that there are no further interferences in the reaction other than the compound evaporation. The validation of the method was achieved by determining the aqueous-phase $\cdot\text{OH}$ -oxidation rate constants for acetone and isopropanol, which have been extensively studied in the literature (Table S1). Both compound decays were monitored in the reactor's headspace with the PTR-MS and their k_{OH} values were determined using Eq. (2). The experiments were triplicated. The uncertainty of the rate constant was calculated by the propagation of the three values standard deviation and the methanol 255 rate constant uncertainty.

Figure 3 compares the experimentally determined k_{OH} values for acetone and for isopropanol in this work with the previous values reported in the literature. The determined rate constants, $1.9 (\pm 0.1) \cdot 10^9 \text{ L mol}^{-1} \text{ s}^{-1}$ for isopropanol, and for acetone, $1.0 (\pm 0.2) \cdot 10^8 \text{ L mol}^{-1} \text{ s}^{-1}$, agree very well with the reported values within the experimental uncertainties.

These results show the relevance of the developed method for accurately determining the aqueous-phase $\cdot\text{OH}$ -oxidation rate 260 constant of any semi-volatile or non-volatile compound detectable either by PTR-MS or by UHPLC-UV. Hereafter, the new rate constants for organic nitrates are presented and discussed.

3.2 New aqueous-phase k_{OH} determinations: application of the kinetic method to organic nitrates

Aqueous-phase k_{OH} for organic nitrates were determined for the first time using the developed competition method. The kinetic rate constants were calculated by Eq. (4) for isobutyl nitrate, 1-pentyl nitrate and isopentyl nitrate and 2-ethylhexyl nitrate; by 265 Eq. (3) for α -nitrooxyacetone, 1-nitrooxy-2-propanol and isosorbide 5-mononitrate; and by Eq. (4) and Eq. (5) for isopropyl nitrate. Figure 4 shows some examples of the linear regressions obtained for each organic nitrate where the slope corresponds to the $k_{OH,X}/k_{OH,M}$ ratio. It evidences the diversity of values obtained for the studied organic nitrates, which all fall within less than an order of magnitude from that of methanol, thus confirming that this reference is appropriate for the studied molecules. The determined aqueous-phase $\cdot\text{OH}$ -oxidation rate constants for the organic nitrates are compiled in Table 2. Uncertainties 270 were calculated by propagating the standard deviation of the replicates with the uncertainty of the methanol k_{OH} rate constant. Then, to account for the small number of experiments performed for some molecules, the uncertainties are given by the confidence limits of 95 % given by the Student's t-distribution. This explains why the value obtained for 1-pentyl nitrate or 2-ethylhexyl nitrate shows the largest uncertainty as its k_{OH} was determined by only two experiments. Data for 2-ethylhexyl nitrate showed inconsistency compared to the other alkyl nitrates (significantly lower value in respect to its chemical structure). 275 It is possible that even with a low initial concentration ($5 \cdot 10^{-5} \text{ mol L}^{-1}$), well below its solubility threshold ($1 \cdot 10^{-4} \text{ mol L}^{-1}$) the complete dissolution of the compound was not achieved when the reaction started, thus inducing an incorrect rate constant value. Furthermore, it is suspected, from its structure, to present some surface activity, thus preventing this compound to dissolve into the bulk water.

Even though there are no other data available in the literature to compare with, the values obtained for the other k_{OH} are 280 consistent regarding the chemical structures: they reflect that the rate constant increases with the number of reactive sites. In

more details, the chemical structure of the organic nitrate and the position of the nitrate group plays an important role on the ·OH-oxidation rate constant. Figure 5a compares these values with the rate constants of their corresponding alcohols and non-functionalized molecules. It shows how the ·OH-oxidation is reduced when the nitrate group (–ONO₂) is replacing an alcohol group (–OH) or a hydrogen (–H). The nitrate group attached to a primary carbon atom (i.e., isobutyl nitrate, 1-pentyl nitrate, 285 isopentyl nitrate, α -nitrooxyacetone and 1-nitrooxy-2-propanol) slows down the reactivity by a factor of 1.7 to 3.1 in comparison to their H-substituted homologues (isobutane, pentane, isopentane, acetone and isopropanol). For isopropyl nitrate, a secondary organic nitrate, the ·OH-attack is reduced by an order of magnitude compared to *n*-propane.

A reduction of the reactivity caused by the presence of the nitrate group also occurs in the gas-phase but in a much slighter manner (Fig. 5b). It has been discussed that the nitrate group has an electron withdrawing nature that strengthens the C–H 290 bond of the α - and the β -carbon atom thus lowering the hydrogen abstraction (Atkinson et al., 1982). However, the reduction of the reactivity is clearly more pronounced in the aqueous-phase, implying a solvent kinetic effect that can more effectively lower the reactivity. This could be induced by the stabilization of the reactant (Koner et al., 2007) or by the formation of a solvent barrier provoked by the nitrate group solvation which could hinder the attack of the hydroxyl radical. The latter inhibiting effect could hinder the ·OH-attack further than the β position, up to the γ position.

295 In order to evaluate this question and to predict the reactivity of other organic nitrates with ·OH radicals in the aqueous-phase, we have investigated a Structure-Activity Relationship (SAR). extended the Structure Activity Relationship method (SAR) initially built by Monod and Doussin, 2008 and Doussin and Monod, 2013 to this class of compounds.

3.3 Structure-Activity Relationship (SAR) for ·OH-oxidation rate constants for organic nitrates

3.3.1 SAR Principles

300 Using the experimentally determined aqueous-phase ·OH-oxidation rate constants, the aqueous-phase SAR previously developed by Monod and Doussin (2008) and Doussin and Monod (2013) was extended to organic nitrates. Briefly, the principle of the estimation assumes that the overall rate constant for the ·OH radical induced H-abstraction is equal to the sum of each kinetic rate of each reactive site. These partial kinetic rate constants are determined by considering the chemical environment of the function along the carbon skeleton. Each –CH₃, –CH₂–, –CH<, –OH and –CHO function of the molecule 305 is associated with a group kinetic rate constant: k(group). To consider both field and resonance effects, the rate constants k associated with each H-bearing function are modulated with both the α -neighboring effect (represented by the F parameters) and the β -neighboring effect (represented by the G parameters). This aqueous-phase SAR can predict the ·OH-oxidation rate constants of alkanes, alcohols, diols, geminal diols, carbonyls, carboxylic acids, carboxylates, and cyclic compounds as well 310 as polyfunctional molecules. For organic nitrates, in addition to the F(–ONO₂) and G(–ONO₂) parameters, one specific parameter, H(–ONO₂) was included to test the influence of the nitrate group on the reactivity on distant reactive sites in γ position, Eq. (6):

$$k = \sum_{i=1}^n (k(i) \cdot \prod F(\alpha\text{-group}) \cdot \prod G(\beta\text{-group}) \cdot \prod H_{ONO_2}(\gamma\text{-group}) \cdot C(cycle)), \quad (6)$$

where $k(i)$ is the partial rate constant for a $-\text{CH}<$, $-\text{CH}_2-$, $-\text{CH}_3$, $-\text{CHO}$ or $-\text{OH}$; $\prod F(\alpha\text{-group}) \cdot G(\beta\text{-group})$ is the product of all the contribution factors of the different neighboring groups for a reactive site in the α and β positions respectively; 315 H_{ONO_2} (γ -group) is the contribution factor specific of the nitrate function for a reactive site in the γ position; and $C(\text{cycle})$ is a contribution factor which represent the cycle effect strains and only affects to reactive positions inside a cycle. Detailed examples where Eq. (6) is applied to calculate the organic nitrates aqueous-phase k_{OH} can be found in S2.

In order to include in this new extended SAR a complex polyfunctional molecule such as isosorbide 5-mononitrate, which comprises two 5-atom cycloether structures, the neighboring effects of ethers and cycloethers have also been determined, i.e.

320 $F(-\text{O}-)$, $G(-\text{O}-)$ and a parameter $X(-\text{O}-)$ used to calculate the cycle effect strains for cycloethers by multiplying the existing $C(\text{cycle})$ factor by a $X(-\text{O}-)$ contribution factor which indicates the presence of one or two oxygen atoms in the cycle.

Furthermore, as all carbonyl compounds, α -nitrooxyacetone can be hydrated in water leading to an equilibrium with its geminal diol form, the equilibrium constant, K_{hyd} , is defined, if water activity is considered as unity, by Eq. (7).

$$K_{\text{hyd}} = \frac{[\text{gem-diol}]}{[\text{carbonyl}]} , \quad (7)$$

325 The reactivity of these partner molecules toward $\cdot\text{OH}$ radicals can be significantly different (Doussin and Monod, 2013), however, the experimental determination only refers to the global rate constant, defined by Eq. (8).

$$k_{\text{overall}} = \frac{K_{\text{hyd}} \cdot k_{\text{gem-diol}} + k_{\text{carbonyl}}}{K_{\text{hyd}} + 1} , \quad (8)$$

where k_{overall} is the overall rate constant for the $\cdot\text{OH}$ -oxidation and $k_{\text{gem-diol}}$ and k_{carbonyl} the calculated rate constants for the related species. When performing the SAR calculation, this equilibrium was considered, and descriptors were proposed to 330 determine both the carbonyl + $\cdot\text{OH}$ and gem-diol + $\cdot\text{OH}$ rate constants and the overall rate constant was calculated to be compared with the experimental data.

Due to the absence of any experimental determination of K_{hyd} in the literature for organic nitrates, a specific experiment was performed to determine the hydration constant of α -nitrooxyacetone. This was done by dissolving the compound in D_2O and measuring the NMR ratios between the signals associated with the geminal diol configuration and the ones associated with the 335 carbonyl form. Details on these experiments as well as the α -nitrooxyacetone NMR spectra are presented in S3. The hydration constant for α -nitrooxyacetone was determined to be $K_{\text{hyd}} = 0.048 \pm 0.002$ at 298 K.

3.3.2 Database for the extended SAR

A dataset of 24 experimental k_{OH} rate constants for linear ethers and 8 for cycloethers from the literature complemented by 7 organic nitrates k_{OH} rate constant determined in this work were used together to determine the contribution factors of each 340 group. Table S4 compiles all compounds with the corresponding values of experimental k_{OH} rate constants and their associated uncertainties. The rate constants of $\cdot\text{OH}$ -oxidation of all mentioned ethers were previously determined using competition kinetic methods. The rate constants were re-calculated considering updated values for the reference compounds. For the latter,

recommended values were chosen in most cases, however, when no recommendation was mentioned in the literature, or when more recent studies were published, average values were calculated discarding the outlier values from the Dixon's Q test
345 (Table S1).

The F, G, H, and X parameters were varied simultaneously using the Microsoft® Excel® Solver routine to solve the multivariate linear regressions in order to minimize the sum of the square difference between calculated and experimental values normalized by the experimental uncertainties Eq. (9).

$$Q = \sum_i \frac{(k_{i,exp} - k_{i,sim})^2}{\sigma_i^2}, \quad (9)$$

350 where $k_{i,exp}$ and $k_{i,sim}$ are respectively the experimental and simulated k_{OH} for compound i , and σ_i is the experimental uncertainty. This target Q value allowed us to give priority, in the simulations, to experimental data determined with low uncertainties, thus improving the reliability of the SAR compared to the previous developments. The experimental uncertainties were determined thoroughly for organic nitrates (section 4.2) and were directly used for the SAR. ~~except for 2 ethylhexyl nitrate which was excluded from the calculations due to the presumption of slow solubilization during the kinetic experiment as mentioned~~.

355 For ethers, the associated experimental uncertainties were recalculated by considering not only the linear plot uncertainties but also the uncertainties associated with the values for the reference compound, using the propagation of uncertainty. For the values reported with no uncertainty, we arbitrarily assigned a 100% uncertainty to prevent from an excessive contribution of unclear determinations. This was the case, for example, for all the determinations reported in the works from Anbar et al., 1966 and Eibenberger, 1980.

360 The preexisting parameters of the SAR were not modified and they were used as reported in Doussin and Monod, (2013) and Monod and Doussin, (2008). To calculate the new parameters, in a first step, a rough estimation of the ether parameters (F(–O), G(–O–), and X(–O–)) was performed using our dataset by starting from different initial conditions. In a second step, a test of different constraints on organic nitrate parameters was performed using the ether parameters estimated in the first step (for isosorbide 5-mononitrate). Due to the restricted database for organic nitrates, constraints were settled on the values of F(–ONO₂), G(–ONO₂) and H(–ONO₂) and five different cases were tested (Table 3) in order to find the best compromise between 365 a minimum number of independent variables and a realistic parameterization of the possible long-range deactivating effects of the nitrate group. The five different cases were developed to investigate if the deactivating effect affects only the reactive sites in α position to the nitrate group (Case 1) or reaches the reactive sites in β position (Case 2 and Case 3) or in γ position (Case 4 and Case 5). In the final step, once the optimal case was selected, all the new parameters were simultaneously adjusted using 370 the whole dataset (Table 4).

3.3.3 SAR Results

The results obtained for the 5 cases tested are shown in Table 3. Different parameters were evaluated in order to choose the optimal case. The correlation slope between the simulated and the experimental k_{OH} rate constants and their correlation

coefficient, the Q values, and the relative difference between the simulated and the experimental rate constant was calculated

375 for each organic nitrate using Eq. (10):

$$\Delta = \frac{k_{exp} - k_{sim}}{k_{exp}}, \quad (10)$$

the sum of all the individual Δ factors is given in Table 3. A value close to 0 indicates the absence of any significant bias.

In all cases, each contribution factor for organic nitrates which was varied resulted in a value lower than 1, and the nearer to the nitrate group the lower the value was obtained, confirming the deactivating effect of the group. Nonetheless, when Cases

380 1, 2 and 5 were run, the calculated value for $F(-\text{ONO}_2)$ dropped to 0, meaning a total suppression of the H-abstraction in the α position, which is unlikely, thus discarding these three cases. In the two remaining cases (3 and 4), the nitrate group impacts

385 on the reactivity up to the β or the γ position, respectively. Most of the evaluation parameters are very similar in both cases, but Case 4 is much less constrained than Case 3 which holds only one variable (Table 3). Case 3 was thus selected as the optimal case. Furthermore, the value obtained for $H(-\text{ONO}_2)$ in Case 4 (0.92) is close to unity, thus showing a very slight

390 influence of the nitrate group in the γ position, and the difference between this value and unity potentially falls in the experimental uncertainties. The results indicate that the impact of the nitrate group on the reactivity towards $\cdot\text{OH}$ radicals only affects the α - and the β -reactive sites. This means that the reduced reactivity (observed in Fig. 5) is caused by the electron withdrawing effect of the nitrate group which is enhanced in the aqueous-phase.

In the final step, using Case 3 constraints, all the new parameters were simultaneously adjusted using the whole dataset, and

395 the results are listed in Table 4. The resulting neighboring factors for organic nitrates are $F(-\text{ONO}_2) = G(-\text{ONO}_2) = 0.17$. For ethers, the results show that $F(-\text{O}-) = 1.10$, a value higher than unity and $G(-\text{O}-) = 0.33$, lower than 1. This reveals an influence similar to the $-\text{OH}$ group, for which $F(-\text{OH}) = 2.10$ and $G(-\text{OH}) = 0.44$. For these groups, the α -position is activating due to a positive mesomeric effect, whereas the β -position is deactivating due to the oxygen electron-withdrawing effect. Furthermore, the resulting value for $X(-\text{O}-) = 1.79$ reflects that the presence of oxygen atoms in a cycle increases the reactivity

400 of the molecule.

Figure 6 shows the correlation between the calculated versus the experimental $k_{\cdot\text{OH}}$ values, and it is compared to the 1:1 regression line. It shows a good linearity covering a wide range of reactivities, over two orders of magnitude.

The efficiency of the proposed extended SAR for organic nitrates, ethers and cycloethers was studied by calculating the relative difference between the simulated and the experimental rate constant (Δ factor, see Eq. (10)). Overall, for 51 % of the experimental values,

405 the efficiency was better than 75 % ($|\Delta| < 0.25$), and better than 60 % ($|\Delta| < 0.4$) for 69 % of experimental values. For organic nitrates, 6 out of the 7 studied molecules presented an efficiency better than 60 %. Compared to the previous versions of the SAR tested for other functional groups (Doussin and Monod, 2013 and Monod and Doussin, 2008) the efficiencies were slightly lower. This may be due to the way the SAR parameters were calculated in this work. While the previous SAR targeted at minimizing Δ for a maximum number of values, in this work, a good efficiency was prioritized for the experimental values

410 with low uncertainties using Eq. (9). Several arguments provide some evidence on the reliability of the application of the SAR

to other compounds: i) there are only a few discrepancies (deviations by a factor of 2) between the experimental and simulated values, even for low-weighted experimental values, ii) the resolved parameters were chemically coherent, iii) a wide range of reactivities was covered (two orders of magnitude) and iv) isosorbide 5-mononitrate presents a highly complex polyfunctional structure (two cycles, two ether, one alcohol and one nitrate groups), the good agreement between its simulated and experimental k_{OH} values (within uncertainties, Table 2) gives some validation of the extended SAR application to polyfunctional compounds.

Due to the restricted database used here to build the extended SAR, the $-ONO_2$ contribution factors could not elucidate the differences between the $F(-ONO_2)$ and $G(-ONO_2)$ contribution factors. We acknowledge that the differences between the two factors may be significant as it happens for the gas-phase reactions (Jenkin et al., 2018). In order to better assess the detailed influence of the nitrate group to each carbon, more experimental determinations of the kinetic rate constants should be done for the reactivity of these compounds in the aqueous-phase. However, as we have found a good agreement between the simulated values and the experimental ones, the present SAR is useful to estimate the importance of aqueous-phase $\cdot OH$ -oxidation for organic nitrates in the atmosphere.

The extended SAR was used to calculate the $\cdot OH$ -oxidation rate constants of several atmospherically relevant compounds, such as hydroxy nitrates, isoprene nitrates, and terpene nitrates. The atmospheric fate of these molecules is discussed in the next section.

4 Atmospheric implications

In light of these results on the aqueous-phase $\cdot OH$ -oxidation of organic nitrates we estimated the importance of these processes in the atmosphere. We used the developed SAR to predict the k_{OH} rate constants of other atmospherically relevant organic nitrates to evaluate if the aqueous-phase $\cdot OH$ -oxidation has a significant role on their atmospheric lifetimes. Some of the evaluated organic nitrates have been detected in field campaigns (Beaver et al., 2012; Li et al., 2018); they are expected products from isoprene or monoterpenes photooxidation (Lee et al., 2014); or they are small polyfunctional nitrates that may be formed by the fragmentation of terpene nitrates or by the oxidation of alkyl nitrates (Picquet-Varrault et al., 2020; Treves and Rudich, 2003). Selecting organic nitrates potentially relevant to atmospheric chemistry, as well as those mentioned in the literature, we listed 49 compounds that were divided into 7 categories depending on their functionalization and chemical structure: 6 alkyl nitrates, 7 hydroxy nitrates, 7 ketonitrates, 5 aldehyde nitrates, 5 nitrooxy carboxylic acids, 7 other polyfunctional nitrates containing more than one oxygenated group, and 12 terpene nitrates corresponding to highly oxidized organic nitrates formed by the oxidation of terpenes, such as α - and β -pinene, limonene and myrcene. Table S5 appends all the studied molecules and their chemical structures and properties under the scenarios studied below.

Inspired by the work of Epstein and Nizkorodov, (2012), considering various aqueous-phase scenarios from cloud/fog conditions to wet aerosols, we evaluated the atmospheric phase partition of these 49 relevant organic nitrates, and we estimated

the importance of the ·OH-oxidation reaction in the aqueous-phase. Finally, the atmospheric multiphase ·OH-oxidation lifetimes of these compounds under cloud/fog conditions were calculated and compared to their gas-phase lifetimes.

4.1 Aqueous- and aerosol-phase partition of organic nitrates

440 The partition of atmospherically relevant organic nitrates between the aqueous-, the gas- and the aerosol-phases was evaluated. The partition between the gas- and the aqueous-phase was calculated using Eq. (11):

$$K_{gas/aq} = \frac{n_{X,gas}}{n_{X,aq}} = \frac{\rho_W}{L_{WC}K_HRT}, \quad (11)$$

where $n_{X,gas}$ and $n_{X,aq}$ are the number of moles of compound X that are present in the gas- and aqueous-phase respectively, ρ_W is the density of water in g m^{-3} , L_{WC} is the liquid water content (LWC) in g m^{-3} , K_H is the effective Henry's Law constant

445 in $\text{mol L}^{-1} \text{ atm}^{-1}$, R is the ideal gas constant $0.082 \text{ atm L mol}^{-1} \text{ K}^{-1}$ and T the temperature in K.

The partition between the gas and the aerosol-phase was calculated using Eq. (12):

$$K_{gas/aer} = \frac{n_{X,gas}}{n_{X,aer}} = \frac{\overline{M}_{aer}\gamma_X P_X^{vap}}{C_{aer}RT}, \quad (12)$$

where $n_{X,aer}$ is the number of moles of compound X that are present in the aerosol-phase, \overline{M}_{aer} is the mean organic molar mass in the aerosol-phase in g mol^{-1} , γ_X the activity coefficient of a compound X, P_X^{vap} its saturation vapor pressure in atm,

450 and C_{aer} the total organic aerosol mass concentration in g m^{-3} . Combining Eq. (11) and Eq. (12), one obtains the fraction of any compound in each phase. The concentration of a compound in each phase depends on the values of K_H and P_X^{vap} .

The partition was studied for two representative atmospheric conditions: i) under typical cloud/fog conditions with a $LWC = 0.35 \text{ g m}^{-3}$ (Fig. 7a); and ii) under wet aerosol conditions with a lower $LWC = 3 \cdot 10^{-5} \text{ g m}^{-3}$ (Fig. 7b) (Herrmann et al., 2015).

455 The aerosol mass concentration was set to $C_{aer} = 1 \cdot 10^{-5} \text{ g m}^{-3}$ with a $\overline{M}_{aer} = 200 \text{ g mol}^{-1}$ and $T = 298 \text{ K}$. The values of K_H were calculated using the SAR developed by Raventos-Duran et al., (2010), and the values of P_X^{vap} were calculated with the

group contribution method by Nannoolal et al., (2004) and Nannoolal et al. (2008). Both values were taken from the GECKO-A website (http://gecko-a.lisa.u-pec.fr/generateur_form.php). The activity coefficient was assumed to be 1 due to the lack of experimental or simulated data, while in a real organic aerosol, γ_X can range from 0.8 to 10 (Wania et al., 2014). It is worth

noting that in the atmosphere, the equilibrium may not be instantaneous. In their kinetic flux model, Shiraiwa and Seinfeld (2012) demonstrate that equilibrium is achieved in the order of seconds or minutes for the phase partitioning of relatively high

volatility organic compounds into liquid particles, while the equilibration timescale ranges from hours to days for semi-solid viscous particles, low volatility species or large particle sizes, and thus can be subject to equilibrium shifts by faster chemical

reactions in each phase. However, these considerations are beyond the scope of the study, as the goal was to determine how aqueous-phase chemistry can affect organic nitrates fate even at very low LWC. Thus, Eq. (12) was used to understand if the

465 partition into the aerosol-phase is important compared to the aqueous-phase and the gas-phase, under the two investigated conditions.

Figure 7 shows the partition of the selected 49 relevant organic nitrates in the three phases. Under cloud/fog conditions ($LWC = 0.35 \text{ g m}^{-3}$, Fig. 7a) all compounds partition between the aqueous-phase (blue) and the gas-phase (red). The presence of terpene nitrates in the aqueous-phase is highly significant: 10 out of the 12 studied molecules are present in the aqueous-phase in proportions higher than 95%. Under the same conditions, small functionalized nitrates (with five carbons or less) partition in both phases depending on their functionalization. No significant partition to the aerosol-phase is observed under these conditions. Under wet aerosol conditions ($LWC = 3 \cdot 10^{-5} \text{ g m}^{-3}$, Fig. 7b) small organic nitrates are only present in the gas-phase (red). High molecular mass compounds such as terpene nitrates equally partition between the aqueous- (blue) and the aerosol-phase (green).

These results show that depending on their reactivity, the compounds which mainly partition into the aqueous-phase may show a different atmospheric lifetime compared to the one assessed if only the gas-phase reactions are considered.

4.2 ·OH-oxidation multiphase lifetimes of organic nitrates

The atmospheric reactivity of each of the 49 organic nitrates with ·OH radicals in the gas-phase was compared to the aqueous-phase one using W value defined in Eq. (13):

$$480 \quad W = \frac{\frac{dn_{X,gas}}{dt}}{\frac{dn_{X,aq}}{dt}} = \frac{\rho_W}{LWC K_H RT} \frac{k_{OH,gas} [OH]_{gas}}{k_{OH,aq} [OH]_{aq}}, \quad (13)$$

where $k_{OH,gas}$ and $k_{OH,aq}$ are the gas-phase and aqueous-phase ·OH-oxidation rate constants respectively in $\text{mol L}^{-1} \text{ s}^{-1}$ (being the volume unit L of air and L of atmospheric water for $k_{OH,gas}$ and $k_{OH,aq}$, respectively). $[OH]_{gas}$ and $[OH]_{aq}$ (in mol L^{-1} of air and mol L^{-1} of atmospheric water, respectively) are the concentrations of hydroxyl radicals in the gas- and the aqueous-phase.

485 Figure 8 compares the ·OH reactivity of organic nitrates in the aqueous- and the gas-phase for cloud/fog conditions (Fig. 8a) and for wet aerosol conditions (Fig. 8b) described in the previous section. The ·OH radical concentrations were set to $1.4 \cdot 10^6 \text{ molecules cm}^{-3}$ ($2.32 \cdot 10^{-15} \text{ mol L}^{-1}$) in the gas-phase and $10^{-14} \text{ mol L}^{-1}$ in the aqueous-phase (Tilgner et al., 2013). The $k_{OH,aq}$ rate constants were calculated using the extended SAR developed in this work (Eq. (6)). Neighboring factors for nitrate and ether groups were those calculated in this work (Table 4) while all other parameters were taken from Doussin and Monod, 490 (2013) and Monod and Doussin (2008). Eq. (8) was employed for compounds containing carbonyl groups. For organic nitrates containing a carboxylic acid functional group, the contributions of both the protonated molecule and its conjugated base were considered. For these compounds, the pH was set to 5 and 3 respectively for cloud/fog conditions and for wet aerosol conditions. The experimental $k_{OH,gas}$ were used when available (references in Fig. 5). They were complemented, when necessary, using the gas-phase SAR developed by Jenkin et al., (2018). The GROHME method was used to obtain the K_{hyd} 495 for compounds containing a carbonyl group (Raventos-Duran et al., 2010). Both the simulated $k_{OH,gas}$ and K_{hyd} were taken from the GECKO-A website (http://gecko.lisa.u-pec.fr/generateur_form.php).

The y-axis of Fig. 8 represents the effective Henry's Law constant for each molecule. The ratio of gas- to aqueous-phase $\cdot\text{OH}$ -oxidation rate constant (in $\text{L of air} \cdot \text{L}^{-1}$ of atmospheric water) is shown in the x-axis. Isopleths show the W values. A W value lower than 1 (blue background) implies that more than 50% of the target compound is consumed in the aqueous-phase. The 500 two dashed isopleths above and below $W = 1$ isopleth represent the limits for aqueous- and gas-phase processing exceeding 95% respectively.

Under cloud/fog conditions (Fig. 8a), most of the studied compounds present an important aqueous-phase processing. Most of the terpene nitrates are highly functionalized and have a high molecular weight, they are almost absent in the gas-phase, and their $\cdot\text{OH}$ -oxidation is solely governed by their aqueous-phase kinetics. Only two terpene nitrates, which are first generation 505 reaction products of α - and β -pinene $\text{NO}_3\cdot$ -oxidation (Li et al., 2018), have a sufficiently low K_H for their $\cdot\text{OH}$ removal to take place mostly in the gas-phase ($\approx 93\%$) due to their low functionalization.

For smaller functionalized organic nitrates, the gas-phase $\cdot\text{OH}$ -oxidation reaction is important. However, one can see that an 510 important fraction of the compounds is located between the dashed isopleths, meaning that both the gas- and the aqueous-phase processing are relevant in their atmospheric loss towards $\cdot\text{OH}$ radicals. This behavior is highly related to the functionalization of the organic nitrate. For small ketonitrates and aldehyde nitrates, their loss is mainly taking place in the gas-phase. With the increase of polarity, such as for hydroxy nitrates, and even more substantially for nitrooxy carboxylic acids, the aqueous-phase $\cdot\text{OH}$ -oxidation becomes more important. For organic nitrates with more than one oxidized group, their processing in the aqueous-phase becomes the major loss process. This observation could be relevant for atmospheric chemistry since some products of isoprene photooxidation are highly functionalized organic nitrates (Fisher et al., 2016).

515 Figure 8b shows the relative importance of aqueous-phase $\cdot\text{OH}$ -oxidation under wet aerosol conditions ($LWC = 3 \cdot 10^{-5} \text{ g m}^{-3}$). Under these conditions, the aqueous-phase $\cdot\text{OH}$ -oxidation is relevant for most of the terpene nitrates. However, under these conditions these compounds should also partition to the aerosol-phase (Fig. 7b). In this phase, not only the $\cdot\text{OH}$ -oxidation kinetic rate constants may differ from the gas and the aqueous-phase ones but also other oxidants, such as singlet oxygen or triplet excited state of dissolved organic matter, can play a crucial role in the atmospheric loss of these compounds (Kaur and 520 Anastasio, 2018; Manfrin et al., 2019). Therefore, this chemistry should be included to precisely evaluate the atmospheric loss of terpene nitrates at these conditions. For small organic nitrates, the gas-phase $\cdot\text{OH}$ -oxidation reaction remains their major loss pathway. Figure 8 shows that most of the compounds for which aqueous-phase is the major loss process, the ratio $k_{\text{OH},\text{gas}}/k_{\text{OH},\text{aq}}$ is higher than 1, thus inducing a slower consumption in the aqueous-phase. This point is specifically investigated in Fig. 9 and in Table S5.

525 Multiphase $\cdot\text{OH}$ -oxidation lifetimes ($\tau_{\text{OH},\text{multiphase}}$) were calculated for each organic nitrate by considering the $\cdot\text{OH}$ reactivity both in the atmospheric aqueous-phase and gas-phase under cloud/fog conditions using Eq. (14):

$$\tau_{\text{OH},\text{multiphase}} = \frac{1}{\Phi_{\text{aq}}k_{\text{OH},\text{aq}}[\text{OH}]_{\text{aq}} + \Phi_{\text{gas}}k_{\text{OH},\text{gas}}[\text{OH}]_{\text{gas}}}, \quad (14)$$

where Φ_{aq} and Φ_{gas} are respectively the fraction of each compound present in the aqueous- and in the gas-phase.

Under cloud/fog conditions, the multiphase ·OH-oxidation lifetimes range from hours to several days and they are compiled in Table S5. Their $\tau_{OH,multiphase}$ is dependent on the chemical structure of the molecules. Large molecules, such as terpene nitrates, or compounds with reactive groups such as aldehyde nitrates show low ·OH-oxidation lifetimes (from 6 to 27 hours). For most of the other organic nitrates, their lifetimes range from 1 day to 1 week, such as primary alkyl nitrates, hydroxy nitrates, ketonitrates with more than 3 carbon atoms or organic nitrates containing more than one different functional group. The last category contains 4 important isoprene-derived nitrates for which multiphase ·OH-oxidation lifetimes are 1 day for C₅ dihydroxy dinitrate, 1 day for methacrolein nitrate and 2 and 4 days for the two isomeric forms of methylvinyl nitrate. The most persistent molecules towards ·OH present are small (≤ 3 carbon atoms), bear reactivity inhibiting functional groups such as carboxylic groups or combine more than one nitrate group. The multiphase ·OH-oxidation lifetimes for these molecules can reach 28 days. Isopropyl nitrate and α -nitrooxyacetone, compounds which have been widely detected in the atmosphere, present very low atmospheric reactivity towards ·OH radicals (24 and 19 days, respectively).

Among the selected organic nitrates, some compounds bear their nitrate group on a tertiary carbon; these species may undergo very fast hydrolysis (Darer et al., 2011; Jacobs et al., 2014). Their lifetimes with respect to hydrolysis range from 1 min to 8.8 h (Takeuchi and Ng, 2019). Therefore, for most of these compounds their hydrolysis is likely the main loss reaction in the atmosphere. Nevertheless, as mentioned in Section 1, the non-hydrolyzable fraction of organic nitrates ranges from 68 to 91 % for α -pinene and β -pinene derived organic nitrates thus for most of these organic nitrates this reaction does not occur.

Photolysis is also a likely sink for organic nitrates, mostly for carbonyl nitrates. Gas-phase photolysis lifetimes have been experimentally determined or simulated for eleven of these compounds and they range from 0.5 to 15 h (Barnes et al., 1993; Müller et al., 2014; Picquet-Varrault et al., 2020; Suarez-Bertoá et al., 2012). At these rates, gas-phase photolysis is expected to be the main chemical loss process for low molecular-weight carbonyl nitrates. On the other hand, to our knowledge, no aqueous-phase photolysis lifetimes have been experimentally determined for carbonyl nitrates. Meanwhile, Romonosky et al. (2015) investigated molar absorptivity of a series of β -hydroxynitrates in the aqueous-phase, and, assuming similar quantum yields as in the gas-phase, they calculated the photolysis rate constant ratios between the gas- and aqueous-phase. Using their approach, aqueous phase photolysis is likely a major sink for water soluble carbonyl nitrates as it likely occurs for most isoprene-derived nitrates. However, their results show that ·OH-oxidation in the aqueous- or the gas-phase is a more significant loss process than photolysis for β -hydroxynitrates. This could be the case for atmospherically relevant species such as C₅ dihydroxy dinitrate or for terpene nitrates. For the latter, their ·OH-oxidation lifetimes fall in the same range as the photolysis lifetimes reported for carbonyl nitrates in the gas-phase thus both processes may be relevant for terpene nitrates including those containing carbonyl groups, but further experimental studies would deserve attention to confirm this.

To assess the impact that aqueous-phase ·OH-oxidation has on organic nitrates lifetimes, the ·OH-oxidation lifetimes relative difference was calculated ($\tau_{OH,dif}$) for each compound using Eq. (15):

$$560 \quad \tau_{OH,dif} \% = \frac{\tau_{OH,multiphase} - \tau_{OH,gas-phase}}{\tau_{OH,gas-phase}} \cdot 100, \quad (15)$$

where $\tau_{OH,multiphase}$ derives from Eq. (14), and $\tau_{OH,gas-phase}$ is the $\cdot\text{OH}$ -oxidation lifetime of a compound considering only the gas-phase. For molecules barely partitioning into the aqueous-phase, $\tau_{OH,dif}$ value is close to zero. For molecules partitioning into the aqueous-phase, a positive (respectively negative) value of $\tau_{OH,dif}$ indicates that the aqueous-phase reactivity increases (respectively decreases) the atmospheric lifetime of the molecule while a negative value implies a faster atmospheric removal via aqueous-phase reactivity.

Figure 9a shows $\tau_{OH,dif}$ for the studied organic nitrates. For the families of compounds such as alkyl nitrates, most of the ketonitrates and aldehyde nitrates, which barely partition into the aqueous-phase, their lifetimes remain unchanged compared to the gas-phase reactivity. Substantial atmospheric loss is expected for hydroxy nitrates, nitrooxy carboxylic acids and organic nitrates with more than one oxidized group as in the case of some isoprene- and terpene- nitrates. Their $\tau_{OH,dif}$ ranges from –

75 % to +155 % implying that their global $\cdot\text{OH}$ -oxidation lifetimes may be either shortened or lengthened when the aqueous-phase is considered, depending on the chemical structure of the molecule. Figure 9 shows that for most of these compounds, especially many terpene nitrates and some polyfunctionalized isoprene nitrates, their atmospheric lifetimes significantly increase (by a factor that can exceed 140%) thus showing that their atmospheric lifetimes should be even longer than what is predicted from gas-phase reactions. This effect might be enhanced considering that aqueous $\cdot\text{OH}$ concentrations might be lower than the one used in Eq. (14), i.e.: $1 \cdot 10^{-14}$ M. This value corresponds to aqueous concentrations of $\cdot\text{OH}$ in polluted/urban cloud droplets (Tilgner et al., 2013). Nevertheless, for remote cloud droplets or wet aerosols, the aqueous $\cdot\text{OH}$ concentration might be 2 to 10 times lower (Arakaki et al., 2013). These lower concentrations would induce an increase of the $\cdot\text{OH}$ -oxidation lifetimes of molecules partitioning into the aqueous-phase.

Figure 9b shows that under wet aerosol conditions, only terpene nitrates $\cdot\text{OH}$ -oxidation lifetimes are affected when considering the aqueous-phase. Under this LWC condition, the proposed terpene nitrates partition both in the aqueous- and the aerosol-phase (Figure 7b). In the aerosol-phase, not only the $\cdot\text{OH}$ -oxidation kinetic rate constants may differ from the gas- and the aqueous-phase ones but also other oxidants can play a crucial role in the atmospheric loss of these compounds (Kaur and Anastasio, 2018; Manfrin et al., 2019). Further studies comprising this reactivity are thus needed to better understand the fate of organic nitrates in all atmospheric phases.

585 5 Conclusions

A new competition kinetic method was developed to accurately determine the aqueous-phase $\cdot\text{OH}$ -oxidation rate constants of low reactivity species such as organic nitrates, using a robust reference compound such as methanol. The method was applied to determine new $\cdot\text{OH}$ -oxidation kinetics of 7 organic nitrates (isopropyl nitrate, isobutyl nitrate, 1-pentyl nitrate, isopentyl nitrate, 2-ethylhexyl nitrate, α -nitrooxyacetone, 1-nitrooxy-2-propanol, isosorbide 5-mononitrate), compounds for which aqueous-phase $\cdot\text{OH}$ -oxidation reaction were investigated for the first time. It was found that the nitrate group provokes an important deactivation of the $\cdot\text{OH}$ -attack, similar to the corresponding gas-phase reactions but enhanced by solvent kinetic effects. A previous developed SAR method was extended to include the nitrate group allowing the prediction of aqueous-phase

kinetics for these atmospherically relevant compounds. The resulting SAR parameters for the nitrate group confirmed the extreme deactivating effect of the nitrate group, up to two adjacent carbon atoms. The achieved SAR was then used to evaluate 595 the multiphase fate of 49 organic nitrates of atmospheric relevance, including hydroxy nitrates, ketonitrates, aldehyde nitrates, nitrooxy carboxylic acids and more functionalized organic nitrates. Among these compounds, polyfunctional organic nitrates were found to be extremely impacted by the aqueous-phase ·OH-oxidation, not only due to their very high water solubility, but also due to their reduced reactivity in this solvent. For 50% of the proposed organic nitrates for which ·OH-reaction occurs 600 mainly in the aqueous-phase (more than 50% of the overall removal) their ·OH-oxidation lifetimes increased by 20% to 155% under cloud/fog conditions. This was even more pronounced for terpene nitrates: for 83% of them, the reactivity towards ·OH occurred mostly (> 98%) in the aqueous-phase under fog/cloud conditions, while for 60% of these terpene nitrates their 605 lifetimes increased by 25% to 140% compared to their gas-phase reactivity. We demonstrate that these effects are of importance under cloud/fog conditions, but also under wet aerosol conditions, especially for the terpene nitrates. These results suggest that considering aqueous-phase ·OH-oxidation reactivity of biogenic organic nitrates is necessary to improve the predictions of their atmospheric fates, transport and should result into a better assessment in the distribution of air pollution, SOA formation and NO_x chemistry.

APPENDIX A: Determining aqueous-phase KOH monitoring the headspace with the PTR-MS

Due to the fact that the organic compounds were diluted in the aqueous-phase, headspace analyses were based on the direct 610 proportionality between water and gas-phase concentrations of the analytes (Karl et al., 2003). Furthermore, the influence of the gas-phase ·OH-oxidation was negligible in our system. Equation (1) can be written as:

$$n \frac{[X]_{0(g)}}{[X]_{t(g)}} = \frac{k_{OH,X}}{k_{OH,M}} \cdot \ln \frac{[M]_{0(g)}}{[M]_{t(g)}}, \quad (A1)$$

where $\ln([X]_{0(g)}/[X]_{t(g)})$ and $\ln([M]_{0(g)}/[M]_{t(g)})$ represent the gas-phase concentration relative decay of respectively the target compound and methanol. The gas-phase relative decay of both methanol and (in some cases) the target compound were monitored by the PTR-MS instrument. The PTR-MS measured quantities in counts-per-second (cps) which can be related to 615 absolute headspace concentrations using Eq. (A2),

$$[X]_g = \frac{1}{k_{R_{rate}} t_{R_{time}}} \cdot \frac{\sum cps(X^+)}{cps(H_3O^+)}, \quad (A2)$$

where $\sum cps(X^+)$ is the sum of the counts-per-second of all the fragments which correspond to compound X; $cps(H_3O^+)$ are the counts-per-second of the hydronium ions that protonate the molecule; $k_{R_{rate}}$ is the protonation rate constant for compound X in the PTR-MS drift tube; and $t_{R_{time}}$ is the time spent by the molecule in the drift tube. Combining Eq. (A1) and Eq. (A2), 620 one obtains Eq. (2).

Author contributions. JMGS developed the experimental kinetic method. NB provided the UV-VIS data for organic nitrates. JMGS and SR developed the UHPLC-UV method for organic nitrates. JM and BTR developed the PTR-MS method for organic nitrates. JLC performed the organic nitrates synthesis and the NMR experiments to obtain the α -nitrooxyacetone K_{hyd}. JMGS and AM built the SAR extension to include nitrate and ether contribution factors. NB and JW significantly contributed to the SAR construction. CMV wrote the code in the GECKO-A model to apply the extended SAR to any molecule. AM and JLC lead the project. JMGS and AM wrote the article with inputs from all coauthors.

Data availability. PTR-MS and UHPLC-UV raw data from the experimental method are available at <https://drive.google.com/drive/folders/1cxPdk58rnGZwkzmGGetWe4AGnww356RB?usp=sharing> (last access: 9 July 2020). Data related to the extended SAR or the atmospheric implications sections can be requested to JMGS (juanmiguelgs93@gmail.com) or to AM (anne-monod@univ-amu.fr).

Competing interests. The authors declare that they have no conflict of interest.

Acknowledgements. This project has received funding from the European Union’s Horizon 2020 research and innovation programme under the Marie Skłodowska-Curie grant agreement No713750. It has been carried out with the financial support of the Regional Council of Provence- Alpes-Côte d’Azur and with the financial support of the A*MIDEX (n° ANR- 11-IDEX-0001-02), funded by the Investissements d’Avenir project funded by the French Government, managed by the French National Research Agency (ANR). This study also received funding from the French CNRS-LEFE-CHAT (Programme National-Les Enveloppes Fluides et l’Environnement-Chimie Atmosphérique – Project “MULTINITRATES”), and from the program ANR-PRCI (ANR-18-CE92-0038-02) – Project “PARAMOUNT”. Finally, the authors thank Richard Valorso for his help using the GECKO-A modelling tool.

References

645 Adams, G. E., Boag, J. W. and Michael, B. D.: Reactions of the hydroxyl radical: Part 2. - Determination of absolute rate constants, *Trans. Faraday Soc.*, 61, 1417–1424, doi:10.1039/TF9656101417, 1965.

Alam, M. S., Rao, B. S. M. and Janata, E.: ·OH reactions with aliphatic alcohols: Evaluation of kinetics by direct optical absorption measurement. A pulse radiolysis study, *Radiat. Phys. Chem.*, 67(6), 723–728, doi:10.1016/S0969-806X(03)00310-4, 2003.

650 Anbar, M., Meyerstein, D. and Neta, P.: Reactivity of aliphatic compounds towards hydroxyl radicals, *J. Chem. Soc. B Phys. Org.*, (0), 742–747, doi:10.1039/J29660000742, 1966.

Aoki, N., Inomata, S. and Tanimoto, H.: Detection of C1-C5 alkyl nitrates by proton transfer reaction time-of-flight mass spectrometry, *Int. J. Mass Spectrom.*, 263(1), 12–21, doi:10.1016/j.ijms.2006.11.018, 2007.

Arakaki, T., Anastasio, C., Kuroki, Y., Nakajima, H., Okada, K., Kotani, Y., Handa, D., Azechi, S., Kimura, T., Tsuhako, A.
655 and Miyagi, Y.: A General Scavenging Rate Constant for Reaction of Hydroxyl Radical with Organic Carbon in Atmospheric
Waters, , doi:10.1021/es401927b, 2013.

Atkinson, R.: Kinetics of the gas-phase reactions of OH radicals with alkanes and cycloalkanes, *Atmos. Chem. Phys.*, 3(6),
2233–2307, doi:10.5194/acp-3-2233-2003, 2003.

Atkinson, R. and Aschmann, S. M.: Rate constants for the reactions of the OH radical with the propyl and butyl nitrates and
660 1-nitrobutane at 298 ± 2 K, *Int. J. Chem. Kinet.*, 21(12), 1123–1129, doi:10.1002/kin.550211205, 1989.

Atkinson, R., Aschmann, S. M., Carter, W. P. L., Winer, A. M. and Pitts, J. N.: Alkyl Nitrate Formation from the NO_x-Air
Photooxidations of C₂-C₈ n-Alkanes, , 587(20), 4563–4569, doi:10.1021/j100220a022, 1982.

Atkinson, R., Baulch, D. L., Cox, R. A., Hampson, R. F., Kerr, J. A. and Troe, J.: Evaluated Kinetic and Photochemical Data
for Atmospheric Chemistry: Supplement IV. IUPAC Subcommittee on Gas Kinetic Data Evaluation for Atmospheric
665 Chemistry, *J. Phys. Chem. Ref. Data*, 21(6), 1125–1568, doi:10.1063/1.555918, 1992.

Atkinson, R., Baulch, D. L., Cox, R. A., Hampson, R. F., Kerr, J. A., Rossi, M. J. and Troe, J.: Evaluated Kinetic,
Photochemical and Heterogeneous Data for Atmospheric Chemistry: Supplement V. IUPAC Subcommittee on Gas Kinetic
Data Evaluation for Atmospheric Chemistry, *J. Phys. Chem. Ref. Data*, 26(3), 521–1011, doi:10.1063/1.556011, 1997.

Barnes, I., Becker, K. H. and Zhu, T.: Near UV absorption spectra and photolysis products of difunctional organic nitrates:
670 Possible importance as NO_x reservoirs, *J. Atmos. Chem.*, 17(4), 353–373, doi:10.1007/BF00696854, 1993.

Beaver, M. R., St. Clair, J. M., Paulot, F., Spencer, K. M., Crounse, J. D., Lafranchi, B. W., Min, K. E., Pusede, S. E.,
Wooldridge, P. J., Schade, G. W., Park, C., Cohen, R. C. and Wennberg, P. O.: Importance of biogenic precursors to the budget
of organic nitrates: Observations of multifunctional organic nitrates by CIMS and TD-LIF during BEARPEX 2009, *Atmos.
Chem. Phys.*, 12(13), 5773–5785, doi:10.5194/acp-12-5773-2012, 2012.

675 Becker, K. H. and Wirtz, K.: Gas phase reactions of alkyl nitrates with hydroxyl radicals under tropospheric conditions in
comparison with photolysis, *J. Atmos. Chem.*, 9(4), 419–433, doi:10.1007/BF00114754, 1989.

Bedjanian, Y., Morin, J. and Romanias, M. N.: Kinetics of the reactions of OH radicals with n-butyl, isobutyl, n-pentyl and 3-
methyl-1-butyl nitrates, *Atmos. Environ.*, 155, 29–34, doi:10.1016/j.atmosenv.2017.02.014, 2017.

Bedjanian, Y., Morin, J. and Romanias, M. N.: Reactions of OH radicals with 2-methyl-1-butyl, neopentyl and 1-hexyl nitrates.
680 Structure-activity relationship for gas-phase reactions of OH with alkyl nitrates: An update, *Atmos. Environ.*, 180, 167–172,
doi:10.1016/j.atmosenv.2018.03.002, 2018.

Clemitschaw, K. C., Williams, J., Rattigan, O. V., Shallcross, D. E., Law, K. S. and Anthony Cox, R.: Gas-phase ultraviolet
absorption cross-sections and atmospheric lifetimes of several C₂-C₅ alkyl nitrates, *J. Photochem. Photobiol. A Chem.*, 102,
117–126, doi:10.1016/S1010-6030(96)04458-9, 1997.

685 Darer, A. I., Cole-Filipiak, N. C., Connor, A. E. O. and Elrod, M. J.: Formation and Stability of Atmospherically Relevant
Isoprene-Derived Organosulfates and Organonitrates, *Environ. Sci. Technol.*, 45, 1895–1902, 2011.

Doussin, J.-F. and Monod, A.: Structure–activity relationship for the estimation of OH-oxidation rate constants of carbonyl

compounds in the aqueous phase, *Atmos. Chem. Phys.*, 13(23), 11625–11641, doi:10.5194/acp-13-11625-2013, 2013.

690 Duncianu, M., David, M., Kartigueyane, S., Cirtog, M., Doussin, J. F. and Picquet-Varrault, B.: Measurement of alkyl and multifunctional organic nitrates by proton-transfer-reaction mass spectrometry, *Atmos. Meas. Tech.*, 10(4), 1445–1463, doi:10.5194/amt-10-1445-2017, 2017.

Eibenberger, J.: Pulse Radiolysis Investigations Concerning the Formation and Oxidation of Organic Radicals in Aqueous Solutions, University of Vienna., 1980.

695 Elliot, A. J. and Simsons, A. S.: Rate constants for reactions of hydroxyl radicals as a function of temperature, *Radiat. Phys. Chem.*, 24(2), 229–231, doi:10.1016/0146-5724(84)90056-6, 1984.

Epstein, S. A. and Nizkorodov, S. A.: A comparison of the chemical sinks of atmospheric organics in the gas and aqueous phase, *Atmos. Chem. Phys.*, 12(17), 8205–8222, doi:10.5194/acp-12-8205-2012, 2012.

700 Fisher, J. A., Jacob, D. J., Travis, K. R., Kim, P. S., Marais, E. A., Miller, C. C., Yu, K., Zhu, L., Yantosca, R. M., Sulprizio, M. P., Mao, J., Wennberg, P. O., Crounse, J. D., Teng, A. P., Nguyen, T. B., Clair, J. M. S., Cohen, R. C., Romer, P., Nault, B. A., Wooldridge, P. J., Jimenez, J. L., Campuzano-Jost, P., Day, D. A., Hu, W., Shepson, P. B., Xiong, F., Blake, D. R., Goldstein, A. H., Misztal, P. K., Hanisco, T. F., Wolfe, G. M., Ryerson, T. B., Wisthaler, A. and Mikoviny, T.: Organic nitrate chemistry and its implications for nitrogen budgets in an isoprene- and monoterpane-rich atmosphere: Constraints from aircraft (SEAC4RS) and ground-based (SOAS) observations in the Southeast US, *Atmos. Chem. Phys.*, 16(9), 5969–5991, doi:10.5194/acp-16-5969-2016, 2016.

705 Getoff, N.: Radiation- and photoinduced degradation of pollutants in water. A comparative study, *Int. J. Radiat. Appl. Instrumentation. Part*, 37(5–6), 673–680, doi:10.1016/1359-0197(91)90166-Y, 1991.

Gligorovski, S., Rousse, D., George, C. H. and Herrmann, H.: Rate constants for the OH reactions with oxygenated organic compounds in aqueous solution, *Int. J. Chem. Kinet.*, 41(5), 309–326, doi:10.1002/kin.20405, 2009.

710 Greenstock, C. L., Ng, M. and Hunt, J. W.: Pulse Radiolysis Studies of Reactions of Primary Species in Water with Nucleic Acid Derivatives, in *Radiation Chemistry*, pp. 397–417., 1968.

Herrmann, H.: Kinetics of Aqueous Phase Reactions Relevant for Atmospheric Chemistry, *Chem. Rev.*, 103(12), 4691–4716, doi:10.1021/cr020658q, 2003.

715 Herrmann, H., Hoffmann, D., Schaefer, T., Bräuer, P. and Tilgner, A.: Tropospheric aqueous-phase free-radical chemistry: Radical sources, spectra, reaction kinetics and prediction tools, *ChemPhysChem*, 11(18), 3796–3822, doi:10.1002/cphc.201000533, 2010.

Herrmann, H., Schaefer, T., Tilgner, A., Styler, S. A., Weller, C., Teich, M. and Otto, T.: Tropospheric Aqueous-Phase Chemistry: Kinetics, Mechanisms, and Its Coupling to a Changing Gas Phase, *Chem. Rev.*, 115(10), 4259–4334, doi:10.1021/cr500447k, 2015.

720 Hu, K. S., Darer, A. I. and Elrod, M. J.: Thermodynamics and kinetics of the hydrolysis of atmospherically relevant organonitrates and organosulfates, *Atmos. Chem. Phys.*, 11(16), 8307–8320, doi:10.5194/acp-11-8307-2011, 2011.

Jacobs, M. I., Burke, W. J. and Elrod, M. J.: Kinetics of the reactions of isoprene-derived hydroxynitrates: gas phase epoxide

formation and solution phase hydrolysis, *Atmos. Chem. Phys.*, 14(17), 8933–8946, doi:10.5194/acp-14-8933-2014, 2014.

Jenkin, M. E., Valorso, R., Aumont, B., Rickard, A. R. and Wallington, T. J.: Estimation of rate coefficients and branching ratios for gas-phase reactions of OH with aliphatic organic compounds for use in automated mechanism construction, *Atmos. Chem. Phys.*, 18(13), 9297–9328, doi:10.5194/acp-18-9297-2018, 2018.

Karl, T., Yeretzian, C., Jordan, A. and Lindinger, W.: Dynamic measurements of partition coefficients using proton-transfer-reaction mass spectrometry (PTR-MS), *Int. J. Mass Spectrom.*, 223–224, 383–395, doi:10.1016/S1387-3806(02)00927-2, 2003.

Kaur, R. and Anastasio, C.: First Measurements of Organic Triplet Excited States in Atmospheric Waters, *Environ. Sci. Technol.*, 52(9), 5218–5226, doi:10.1021/acs.est.7b06699, 2018.

Kiendler-Scharr, A., Mensah, A. A., Fries, E., Topping, D., Nemitz, E., Prevot, A. S. H., Äijälä, M., Allan, J., Canonaco, F., Canagaratna, M., Carbone, S., Crippa, M., Dall Osto, M., Day, D. A., De Carlo, P., Di Marco, C. F., Elbern, H., Eriksson, A., Freney, E., Hao, L., Herrmann, H., Hildebrandt, L., Hillamo, R., Jimenez, J. L., Laaksonen, A., McFiggans, G., Mohr, C., O'Dowd, C., Otjes, R., Ovadnevaite, J., Pandis, S. N., Poulain, L., Schlag, P., Sellegri, K., Swietlicki, E., Tiitta, P., Vermeulen, A., Wahner, A., Worsnop, D. and Wu, H. C.: Ubiquity of organic nitrates from nighttime chemistry in the European submicron aerosol, *Geophys. Res. Lett.*, 43(14), 7735–7744, doi:10.1002/2016GL069239, 2016.

Koner, A. L., Pischel, U. and Nau, W. M.: Kinetic solvent effects on hydrogen abstraction reactions, *Org. Lett.*, 9(15), 2899–2902, doi:10.1021/ol071165g, 2007.

Lee, A. K. Y., Adam, M. G., Liggio, J., Li, S.-M., Li, K., Willis, M. D., Abbatt, J. P. D., Tokarek, T. W., Odame-Ankrah, C. A., Osthoff, H. D., Strawbridge, K. and Brook, J. R.: A large contribution of anthropogenic organo-nitrates to secondary organic aerosol in the Alberta oil sands, *Atmos. Chem. Phys.*, 19, 12209–12219, doi:10.5194/acp-19-12209-2019, 2019.

Lee, L., Teng, A. P., Wennberg, P. O., Crounse, J. D. and Cohen, R. C.: On rates and mechanisms of OH and O₃ reactions with isoprene-derived hydroxy nitrates, *J. Phys. Chem. A*, 118(9), 1622–1637, doi:10.1021/jp4107603, 2014.

Li, R., Wang, X., Gu, R., Lu, C., Zhu, F., Xue, L., Xie, H., Du, L., Chen, J. and Wang, W.: Identification and semi-quantification of biogenic organic nitrates in ambient particulate matters by UHPLC/ESI-MS, *Atmos. Environ.*, 176, 140–147, doi:10.1016/j.atmosenv.2017.12.038, 2018.

Lindinger, W., Hansel, A. and Jordan, A.: Proton-transfer-reaction mass spectrometry (PTR-MS): On-line monitoring of volatile organic compounds at pptv levels, *Chem. Soc. Rev.*, 27(5), 347–354, doi:10.1039/a827347z, 1998.

Liu, S., Shilling, J. E., Song, C., Hiranuma, N., Zaveri, R. A. and Russell, L. M.: Hydrolysis of organonitrate functional groups in aerosol particles, *Aerosol Sci. Technol.*, 46(12), 1359–1369, doi:10.1080/02786826.2012.716175, 2012.

Manfrin, A., Nizkorodov, S. A., Malecha, K. T., Getzinger, G. J., McNeill, K. and Borduas-Dedekind, N.: Reactive Oxygen Species Production from Secondary Organic Aerosols: The Importance of Singlet Oxygen, *Environ. Sci. Technol.*, 53(15), 8553–8562, doi:10.1021/acs.est.9b01609, 2019.

Monod, A. and Doussin, J. F.: Structure-activity relationship for the estimation of OH-oxidation rate constants of aliphatic organic compounds in the aqueous phase: alkanes, alcohols, organic acids and bases, *Atmos. Environ.*, 42(33), 7611–7622, 2008.

doi:10.1016/j.atmosenv.2008.06.005, 2008.

Monod, A., Poulain, L., Grubert, S., Voisin, D. and Wortham, H.: Kinetics of OH-initiated oxidation of oxygenated organic compounds in the aqueous phase: New rate constants, structure-activity relationships and atmospheric implications, *Atmos. Environ.*, 39(40), 7667–7688, doi:10.1016/j.atmosenv.2005.03.019, 2005.

760 Motohashi, N. and Saito, Y.: Competitive Measurement of Rate Constants for Hydroxyl Radical Reactions Using Radiolytic Hydroxylation of Benzoate, *Chem. Pharm. Bull.*, 41(10), 1842–1845, doi:10.1248/cpb.41.1842, 1993.

Müller, J. F., Peeters, J. and Stavrakou, T.: Fast photolysis of carbonyl nitrates from isoprene, *Atmos. Chem. Phys.*, 14(5), 2497–2508, doi:10.5194/acp-14-2497-2014, 2014.

765 Nannoolal, Y., Rarey, J., Ramjugernath, D. and Cordes, W.: Estimation of pure component properties: Part 1. Estimation of the normal boiling point of non-electrolyte organic compounds via group contributions and group interactions, *Fluid Phase Equilib.*, 226(1–2), 45–63, doi:10.1016/j.fluid.2004.09.001, 2004.

Nannoolal, Y., Rarey, J. and Ramjugernath, D.: Estimation of pure component properties part 3. Estimation of the vapor pressure of non-electrolyte organic compounds via group contribution and group interactions, *Fluid Phase Equilib.*, 269(1–2), 117–133, doi:10.1016/j.fluid.2008.04.020, 2008.

770 Neyens, E. and Baeyens, J.: A review of classic Fenton's peroxidation as an advanced oxidation technique, *J. Hazard. Mater.*, 98(1–3), 33–50, doi:10.1016/S0304-3894(02)00282-0, 2003.

Picquet-Varraut, B., Suarez-Bertoa, R., Duncianu, M., Cazaunau, M., Pangui, E., David, M. and Doussin, J. F.: Photolysis and oxidation by OH radicals of two carbonyl nitrates: 4-nitrooxy-2-butanone and 5-nitrooxy-2-pentanone, *Atmos. Chem. Phys.*, 20(1), 487–498, doi:10.5194/acp-20-487-2020, 2020.

775 Raventos-Duran, T., Camredon, M., Valorso, R., Mouchel-Vallon, C. and Aumont, B.: Structure-activity relationships to estimate the effective Henry's law constants of organics of atmospheric interest, *Atmos. Chem. Phys.*, 10(16), 7643–7654, doi:10.5194/acp-10-7643-2010, 2010.

Reuvers, A. P., Greenstock, C. L., Borsa, J. and Chapman, J. D.: Studies on the mechanism of chemical radioprotection by dimethyl sulphoxide, *Int. J. Radiat. Biol.*, 24(5), 533–536, doi:10.1080/09553007314551431, 1973.

780 Romer Present, P. S., Zare, A. and Cohen, R. C.: The changing role of organic nitrates in the removal and transport of NO_x, *Atmos. Chem. Phys.*, 20(1), 267–279, doi:10.5194/acp-20-267-2020, 2020.

Romonosky, D. E., Nguyen, L. Q., Shemesh, D., Nguyen, T. B., Epstein, S. A., Martin, D. B. C., Vanderwal, C. D., Gerber, R. B. and Nizkorodov, S. A.: Absorption spectra and aqueous photochemistry of β -hydroxyalkyl nitrates of atmospheric interest, *Mol. Phys.*, 113(15–16), 2179–2190, doi:10.1080/00268976.2015.1017020, 2015.

785 Rudakov, E. S., Volkova, L. K. and Tret'yakov, V. P.: Low selectivity of reactions of OH-radicals with alkanes in aqueous solution, *React. Kinet. Catal. Lett.*, 16, 33–337, 1981.

Sander, R.: Compilation of Henry's law constants (version 4.0) for water as solvent, *Atmos. Chem. Phys.*, 15(8), 4399–4981, doi:10.5194/acp-15-4399-2015, 2015.

Schaefer, T., Schindelka, J., Hoffmann, D. and Herrmann, H.: Laboratory kinetic and mechanistic studies on the OH-initiated

790 oxidation of acetone in aqueous solution, *J. Phys. Chem. A*, 116(24), 6317–6326, doi:10.1021/jp2120753, 2012.

Shiraiwa, M. and Seinfeld, J. H.: Equilibration timescale of atmospheric secondary organic aerosol partitioning, *Geophys. Res. Lett.*, 39(24), doi:10.1029/2012GL054008, 2012.

Suarez-Bertoa, R., Picquet-Varrault, B., Tamas, W., Pangui, E. and Doussin, J. F.: Atmospheric fate of a series of carbonyl nitrates: Photolysis frequencies and OH-oxidation rate constants, *Environ. Sci. Technol.*, 46(22), 12502–12509, 795 doi:10.1021/es302613x, 2012.

Takeuchi, M. and Ng, N. L.: Chemical composition and hydrolysis of organic nitrate aerosol formed from hydroxyl and nitrate radical oxidation of α -pinene and β -pinene, *Atmos. Chem. Phys.*, 19, 12749–12766, doi:10.5194/acp-19-12749-2019, 2019.

Talukdar, R. K., Burkholder, J. B., Hunter, M., Gilles, M. K., Roberts, J. M. and Ravishankara, A. R.: Atmospheric fate of several alkyl nitrates: Part 2. UV absorption cross-sections and photodissociation quantum yields, *J. Chem. Soc. - Faraday Trans.*, 93(16), 2797–2805, doi:10.1039/a701781b, 1997.

800 Thomas, J. K.: Rates of reaction of the hydroxyl radical, *Trans. Faraday Soc.*, 61, 702–707, doi:10.1039/tf9656100702, 1965.

Tilgner, A., Bräuer, P., Wolke, R. and Herrmann, H.: Modelling multiphase chemistry in deliquescent aerosols and clouds using CAPRAM3.0i, *J. Atmos. Chem.*, 70(3), 221–256, doi:10.1007/s10874-013-9267-4, 2013.

Treves, K. and Rudich, Y.: The atmospheric fate of C3-C6 hydroxyalkyl nitrates, *J. Phys. Chem. A*, 107(39), 7809–7817, 805 doi:10.1021/jp035064l, 2003.

Wängberg, I., Barnes, I. and Becker, K. H.: Atmospheric chemistry of bifunctional cycloalkyl nitrates, *Chem. Phys. Lett.*, 261(1–2), 138–144, doi:10.1016/0009-2614(96)00857-3, 1996.

810 Wania, F., Lei, Y. D., Wang, C., Abbatt, J. P. D. and Goss, K.-U.: Novel methods for predicting gas-particle partitioning during the formation of secondary organic aerosol, *Atmos. Chem. Phys. Discuss.*, 14, 21341–21385, doi:10.5194/acpd-14-21341-2014, 2014.

Williams, J. A., Cooper, W. J., Mezyk, S. P. and Bartels, D. M.: Absolute rate constants for the reaction of the hydrated electron, hydroxyl radical and hydrogen atom with chloroacetones in water, *Radiat. Phys. Chem.*, 65(4–5), 327–334, doi:10.1016/S0969-806X(02)00351-1, 2002.

Willson, R. L., Greenstock, C. L., Adams, G. E., Wageman, R. and Dorfman, L. M.: The standardization of hydroxyl radical rate data from radiation chemistry, *Int. J. Radiat. Phys. Chem.*, 3(3), 211–220, doi:10.1016/0020-7055(71)90023-4, 1971.

Wolfenden, B. S. and Willson, R. L.: Radical-cations as reference chromogens in kinetic studies of one-electron transfer reactions: Pulse radiolysis studies of 2,2'-azinobis-(3- ethylbenzthiazoline-6-sulphonate), *J. Chem. Soc. Perkin Trans. 2*, (7), 805–812, doi:10.1039/p29820000805, 1982.

Zhu, T., Barnes, I. and Becker, K. H.: Relative-rate study of the gas-phase reaction of hydroxy radicals with difunctional 820 organic nitrates at 298 K and atmospheric pressure, *J. Atmos. Chem.*, 13(3), 301–311, doi:10.1007/BF00058137, 1991.

Name	Structure	$K_{H, 298\text{ K}} / \text{mol L}^{-1} \text{ atm}^{-1}$	Solubility at 298 K / mol L ⁻¹	Monitored by
Isopropyl nitrate		0.75	$2.5 \cdot 10^{-2}$	PTR-MS
				UHPLC-UV
Isobutyl nitrate		0.60	$9.4 \cdot 10^{-3}$	PTR-MS
1-Pentyl nitrate		0.74	$2.7 \cdot 10^{-3}$	PTR-MS
Isopentyl nitrate		0.40	$2.5 \cdot 10^{-3}$	PTR-MS
2-Ethylhexyl nitrate		0.18	$1 \cdot 10^{-4}$	PTR-MS
α-Nitrooxyacetone		$1.0 \cdot 10^3$	1.6	UHPLC-UV
1-Nitrooxy-2-propanol		$6.7 \cdot 10^4$	0.6	UHPLC-UV
Isosorbide 5-mononitrate		$1.3 \cdot 10^7$	0.3	UHPLC-UV
Isopropanol		130	16.6	PTR-MS
Acetone		30	17.2	PTR-MS

Table 1: Chemical structures and properties of the studied organic nitrates. Henry's Law constants were obtained from Sander, 2015 except for 2-ethylhexyl nitrate and isosorbide 5-mononitrate which were calculated using the SAR developed by Raventos-Duran et al., (2010). Organic nitrates solubilities were calculated using the model WSKOWWIN™.

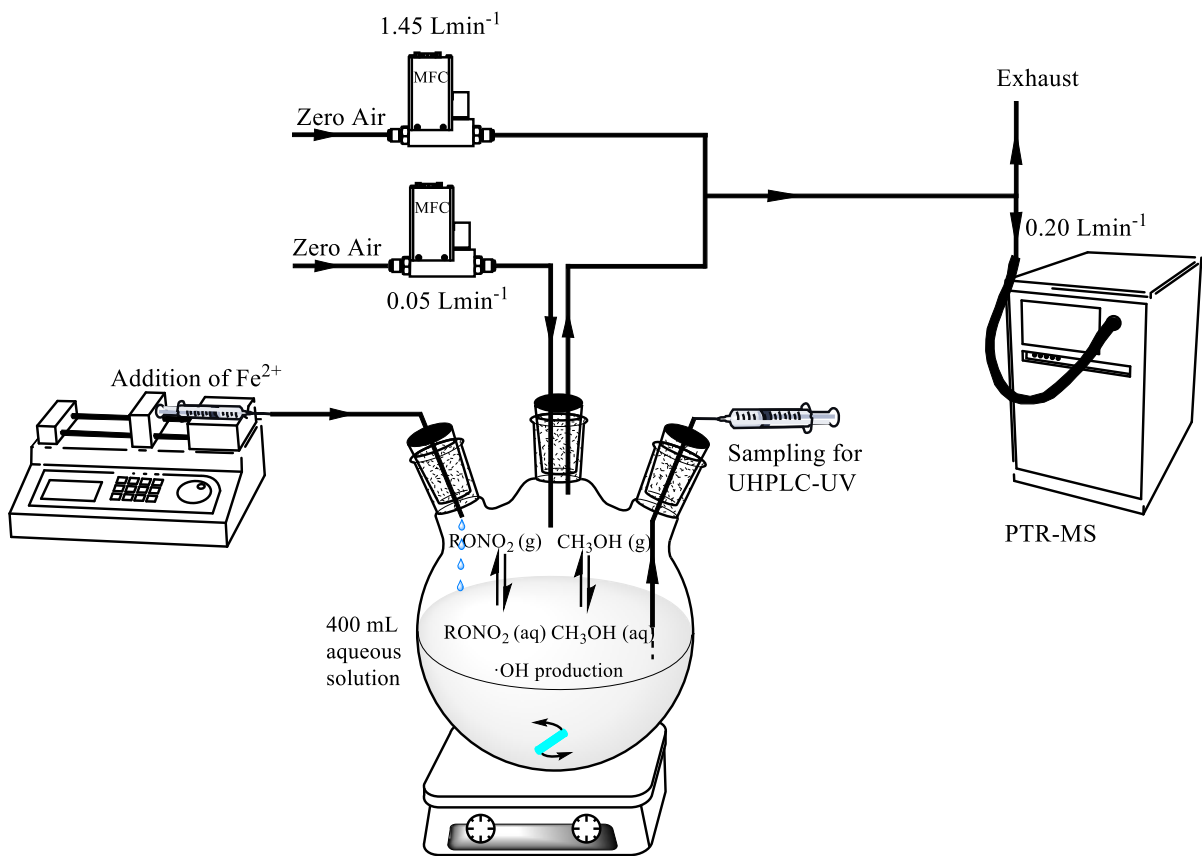


Figure 1: Experimental set-up for the competition kinetics method

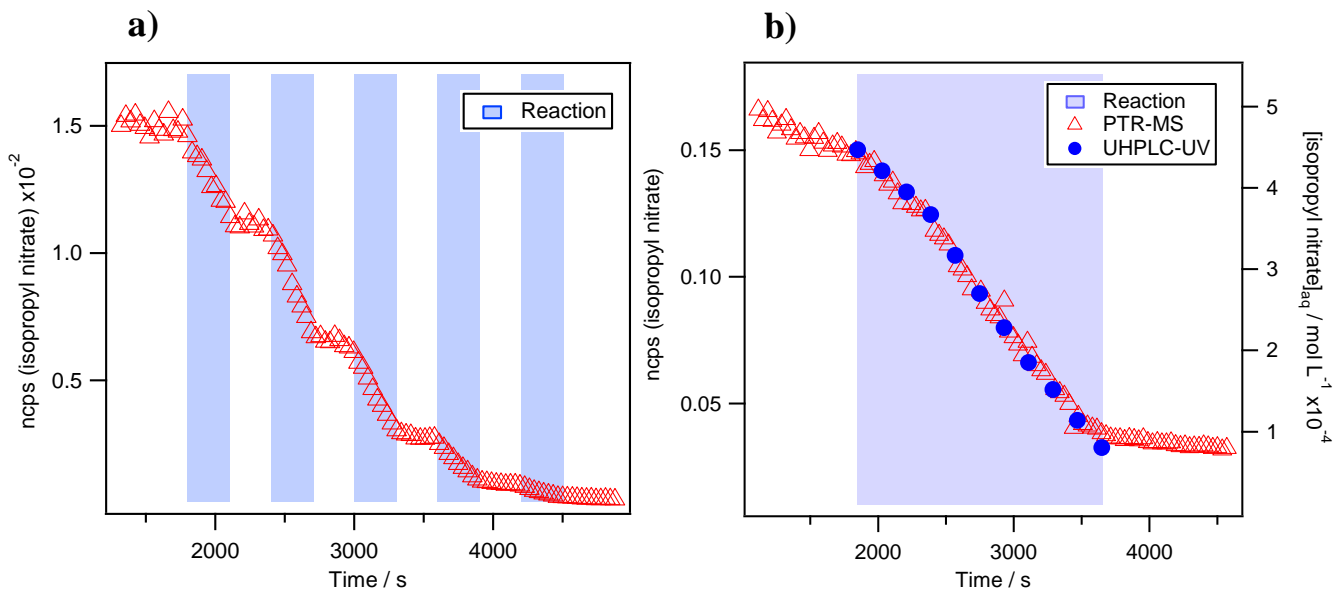


Figure 2: Kinetic decays of isopropyl nitrate during its aqueous-phase ·OH-oxidation a) Monitored by PTR-MS during several sequential additions of the Fe^{2+} solution. Initial conditions in the reactor were $[\text{Isopropyl nitrate}]_0 = 5 \cdot 10^{-5} \text{ mol L}^{-1}$, $[\text{H}_2\text{O}_2]_0 = 4 \cdot 10^{-3} \text{ mol L}^{-1}$ and $[\text{H}_2\text{SO}_4]_0 = 5 \cdot 10^{-3} \text{ mol L}^{-1}$; b) Intercomparison between PTR-MS and UHPLC-UV detection. Initial conditions were $[\text{Isopropyl nitrate}]_0 = 6 \cdot 10^{-4} \text{ mol L}^{-1}$, $[\text{CH}_3\text{OH}]_0 = 3 \cdot 10^{-4} \text{ mol L}^{-1}$, $[\text{H}_2\text{O}_2]_0 = 4 \cdot 10^{-3} \text{ mol L}^{-1}$ and $[\text{H}_2\text{SO}_4]_0 = 5 \cdot 10^{-3} \text{ mol L}^{-1}$. In both graphs the time is set to 0 when isopropyl nitrate is injected. Blue background indicates periods when the solution of Fe^{2+} (0.06 M) was dripped into the reactor to produce ·OH radicals.

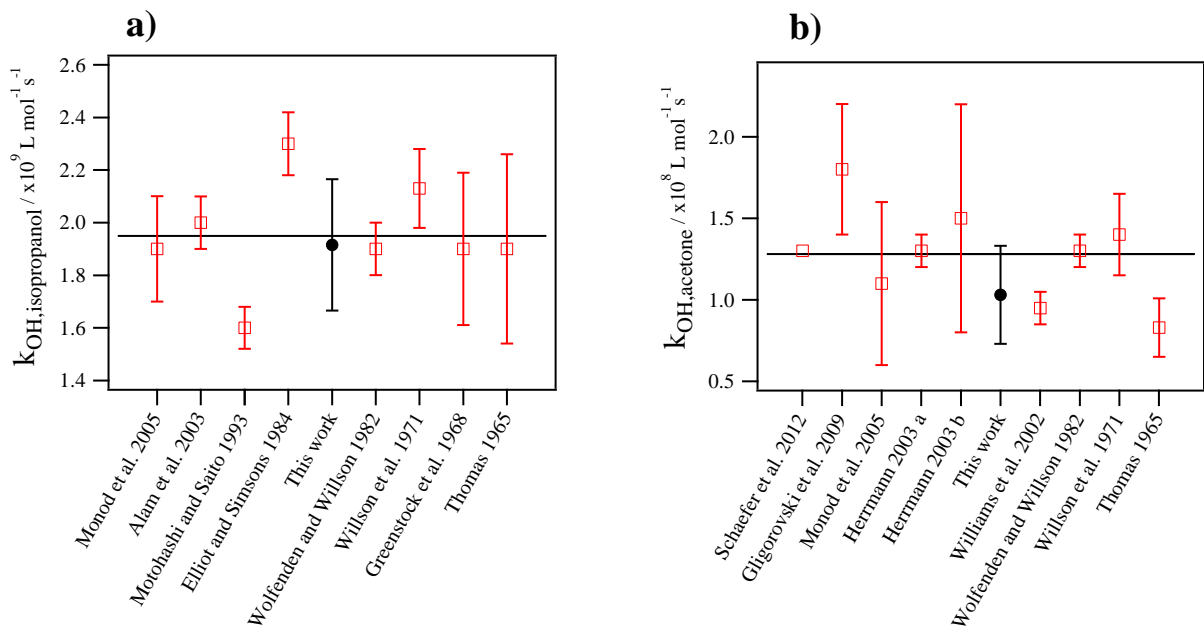


Figure 3: Validation experiments: determination of the aqueous-phase k_{OH} values using the new developed method, and comparison with the reported values in the literature for a) isopropanol and b) acetone. The horizontal line represents the average value of the previous studies.

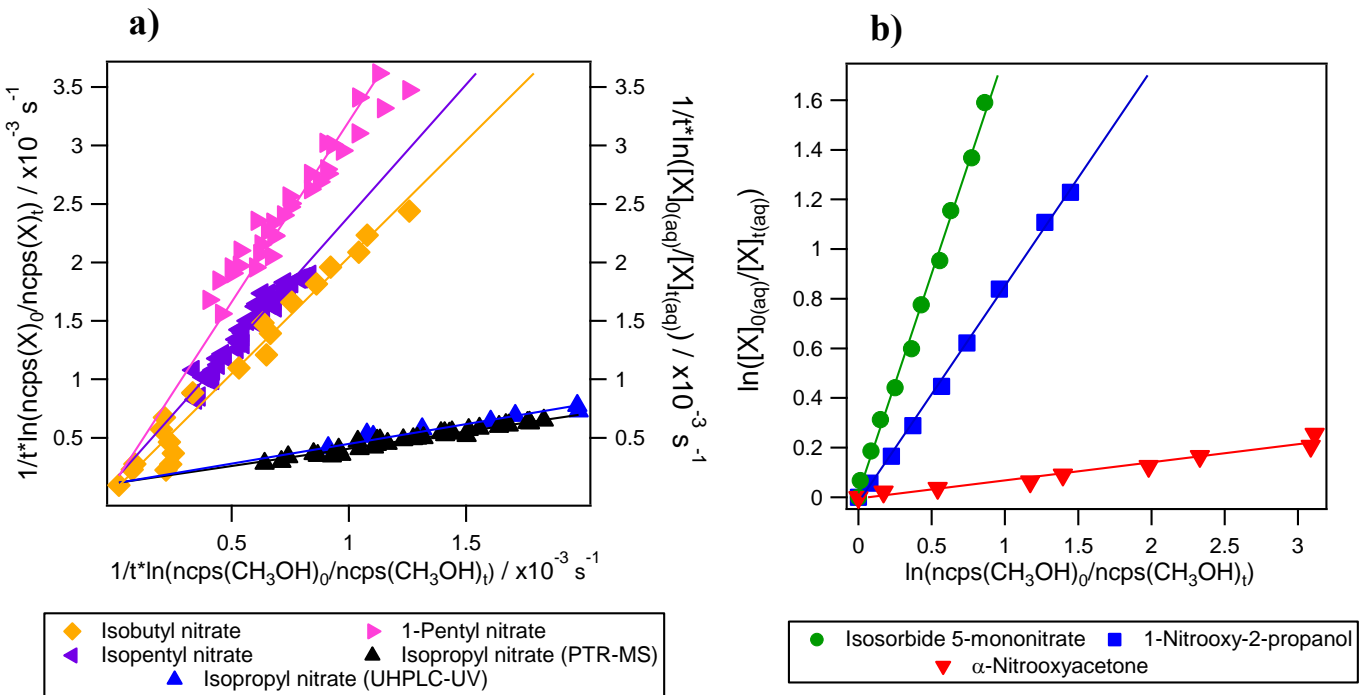


Figure 4: Examples of competition kinetic results for the studied organic nitrates using the new developed method: experiments 8, 14, 16, 19, 21, 24 and 26 (listed in Table S2). In panel a) molecules were monitored in the reactor's headspace by PTR-MS (left axis and horizontal axis) except for isopropyl nitrate which was also monitored by UHPLC-UV (right axis). In panel b) methanol was monitored in the reactor's headspace by PTR-MS (horizontal axis) while the polyfunctional organic nitrates were followed by UHPLC-UV (left axis).

Studied compounds	$k_{OH\ exp}$ / $\cdot 10^8 \text{ L mol}^{-1} \text{ s}^{-1}$	$k_{OH\ sim}$ / $\cdot 10^8 \text{ L mol}^{-1} \text{ s}^{-1}$	Δ	n
Isopropyl nitrate	2.8 (± 0.6)	3.0	-0.07	9
Isobutyl nitrate	17 (± 11)	13.5	+0.22	3
1-Pentyl nitrate	31 (± 46)	31.8	-0.02	2
Isopentyl nitrate	22 (± 9)	24.6	-0.10	3
α -Nitrooxyacetone	0.8 (± 0.4)	1.3	-0.69	3
1-Nitrooxy-2-propanol	8.7 (± 1.9)	6.3	+0.28	3
Isosorbide 5-mononitrate	18 (± 5)	14.2	+0.19	3

850

Table 2: Aqueous-phase $\cdot\text{OH}$ -oxidation rate constants for eight organic nitrates: comparison between the experimental rate constants ($k_{OH\ exp}$) and the simulated ones ($k_{OH\ sim}$) using the extended SAR. Calculations use the SAR parameters indicated in Table 4. The factor Δ is the relative difference between the simulated and the experimental rate constant (Eq. 10). n stands for the number of experimental determinations of each rate constant (note that for isopropyl nitrate 6 experiments were performed, in 3 of them the value was determined twice using both Eq. (4) and Eq. (5) thus resulting in 9 determinations). Experimental uncertainties are 95 % confidence interval.

855

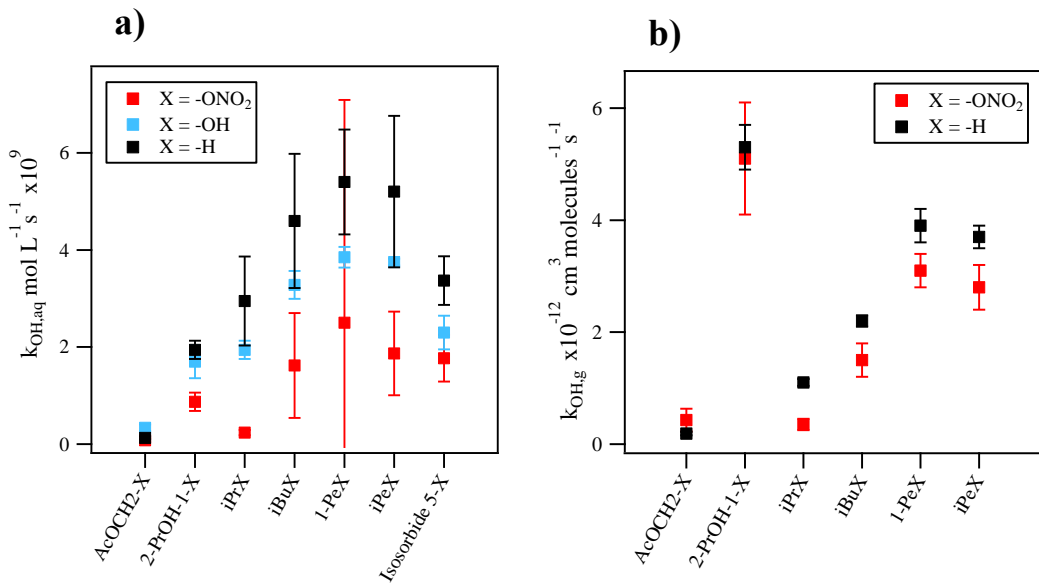


Figure 5: Comparison between the k_{OH} values for organic nitrates, the corresponding alcohols, and non-substituted homologue compounds a) in the aqueous-phase and b) in the gas-phase. Aqueous-phase k_{OH} values were taken from : Reuvers et al., (1973) and Adams et al., (1965) for alcohols; Getoff, (1991) and Rudakov et al., (1981) for H-substituted compounds; the predictions using the SAR for hydroxy acetone and for the -OH and -H substituted homologues of isosorbide 5-mononitrate. Gas-phase k_{OH} values were taken from Atkinson et al., (1982); Atkinson and Aschmann, (1989); Becker and Wirtz, (1989); Bedjanian et al., (2017); Suarez-Bertoa et al., (2012); Talukdar et al., (1997); Treves and Rudich, (2003) and Zhu et al., (1991) for organic nitrates; and from Atkinson et al., (1997), Atkinson et al. (1992); and Atkinson, (2003) for H-substituted homologues.

	Case 1	Case 2	Case 3	Case 4	Case 5
F(–ONO₂)	0	0	0.17	0.18	0
G(–ONO₂)	1*	0.33	0.17	0.18	0.37
H(–ONO₂)	1*	1*	1*	0.92	0.37
Slope	1.18	1.18	1.01	0.98	0.53
R²	0.92	0.97	0.96	0.95	0.94
Δ	-5.19	-0.14	-0.19	0.05	2.06
Q	23.0	0.12	0.59	0.58	0.93
Efficiency 75%	29 %	86 %	71 %	57 %	14 %
Efficiency 60%	43 %	100 %	86 %	86 %	43 %

Table 3: SAR tests on organic nitrate parameters: 5 case tests investigated to evaluate the nitrate group influences. Constraints imposed: Values fixed to 1 (i.e. no influence on the reactivity) marked by *; F(–ONO₂)=G(–ONO₂) for Case 3 and Case 4; and G(–ONO₂)=H(–ONO₂) for Case 5. In bold is the selected case. Slope is the correlation slope between the simulated and the experimental k_{OH} rate constants and R² is the corresponding correlation coefficient. The Δ factor is the relative difference between the simulated and the experimental rate constant. Q is the sum of the square difference between calculated and experimental values normalized by the experimental uncertainties. Efficiencies at 75% and 60% represent the percentage of organic nitrates with $|\Delta| < 0.25$ and $|\Delta| < 0.40$ respectively.

Parameter	Value
F(–O–)	1.10
G(–O–)	0.33
C'5(cycle)	1.43
C'6(cycle)	1.79
F(–ONO₂)	0.17
G(–ONO₂)	0.17

Table 4: SAR results: new calculated neighboring effects parameters for ethers, cyclic ethers and organic nitrates (using Case 3 constraints).

875

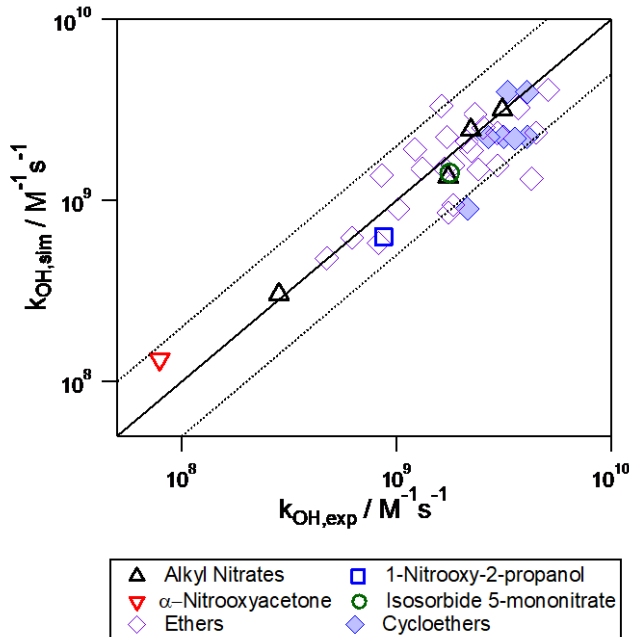


Figure 6: Correlation plot between the experimental and the simulated aqueous-phase $\cdot\text{OH}$ -oxidation rate constants for organic nitrates and ethers. The plain line corresponds to the 1:1 regression and the dashed lines represent the limits where the simulated rate constants deviate from the experimental ones by a factor of 2.

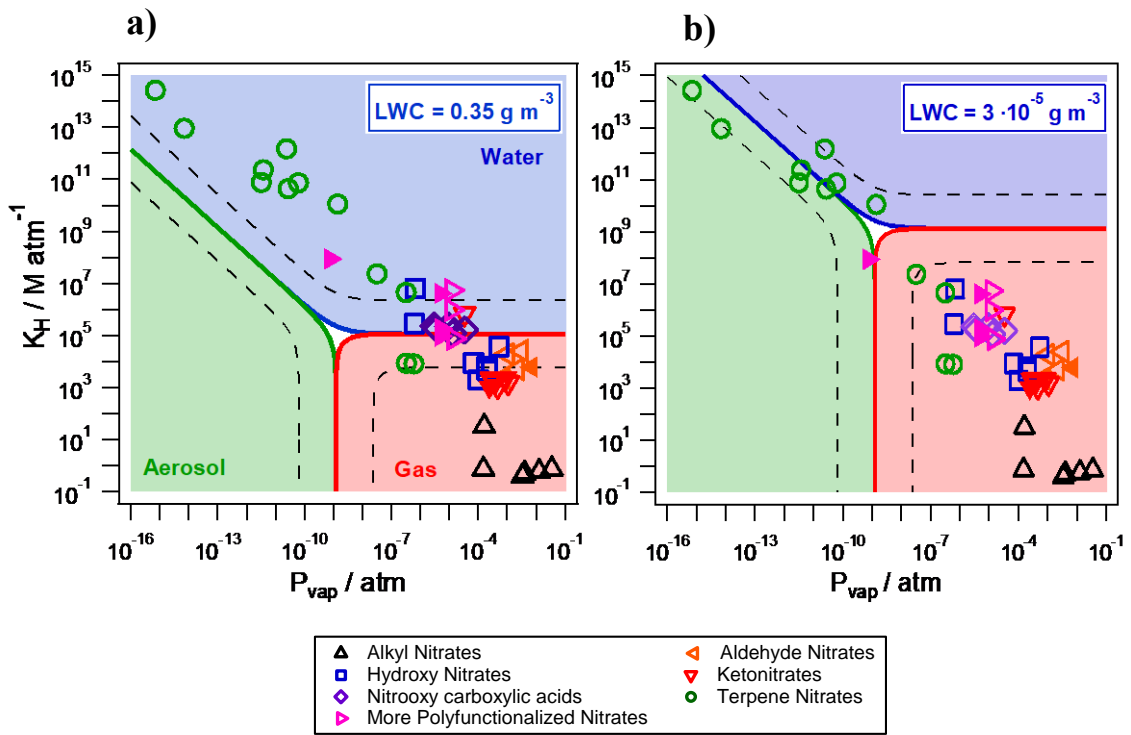


Figure 7: Partition of atmospherically relevant organic nitrates in the aqueous- (blue), the gas- (red) and the aerosol-phase (green) for two different air parcels with a) $\text{LWC} = 0.35 \text{ g m}^{-3}$ (cloud/fog conditions) and b) $\text{LWC} = 3.5 \cdot 10^{-5} \text{ g m}^{-3}$ (wet aerosol conditions). Temperature was set to 298 K, the aerosol mass concentration to $C_{\text{aer}} = 1 \cdot 10^{-5} \text{ g m}^{-3}$ with a $\overline{M}_{\text{aer}} = 200 \text{ g mol}^{-1}$. The dashed lines represent the limits where the concentration of one compound exceeds 95 % in each phase. Filled markers represent organic nitrates derived from isoprene.

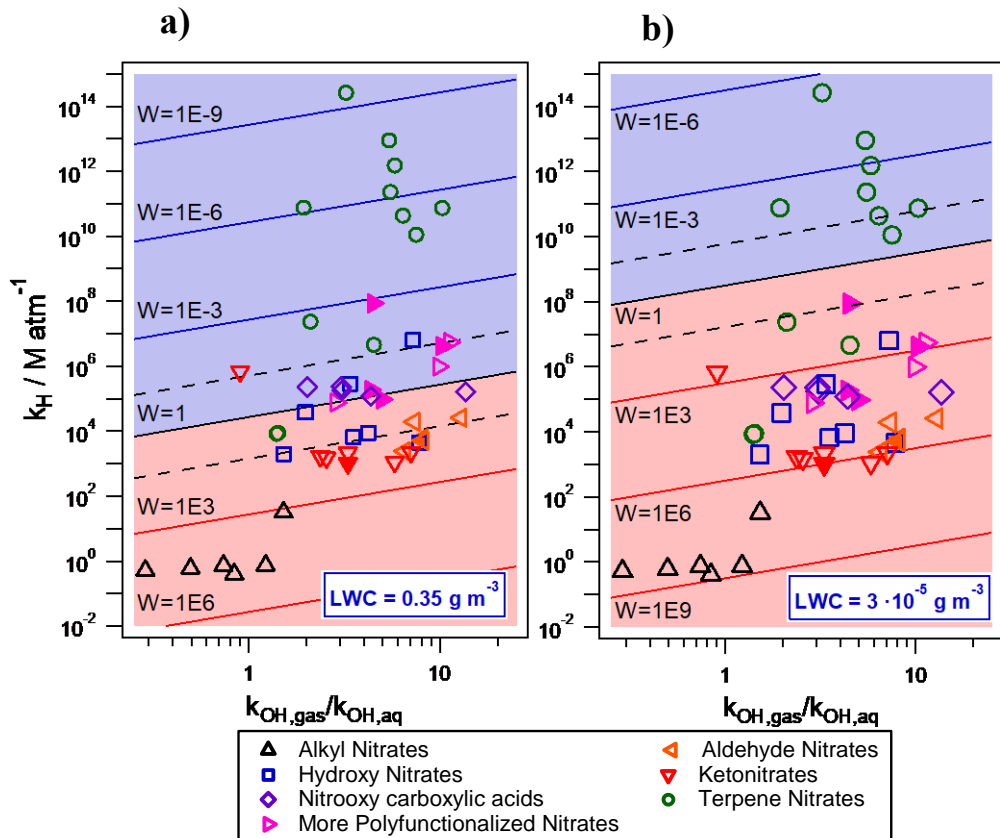


Figure 8: Gas-aqueous partition and reactivity (towards $\cdot\text{OH}$ -oxidation) of 49 organic nitrates for two different air parcels with a) $\text{LWC} = 0.35 \text{ g m}^{-3}$ (cloud/fog conditions) and b) $\text{LWC} = 3.5 \cdot 10^{-5} \text{ g m}^{-3}$ (wet aerosol conditions) at 298 K. $\cdot\text{OH}$ radical concentrations were set to $2.32 \cdot 10^{-15} \text{ mol L}^{-1}$ ($1.4 \cdot 10^6 \text{ molecules cm}^{-3}$) in the gas-phase and to $10^{-14} \text{ mol L}^{-1}$ in the aqueous-phase. Filled markers represent organic nitrates derived from isoprene.

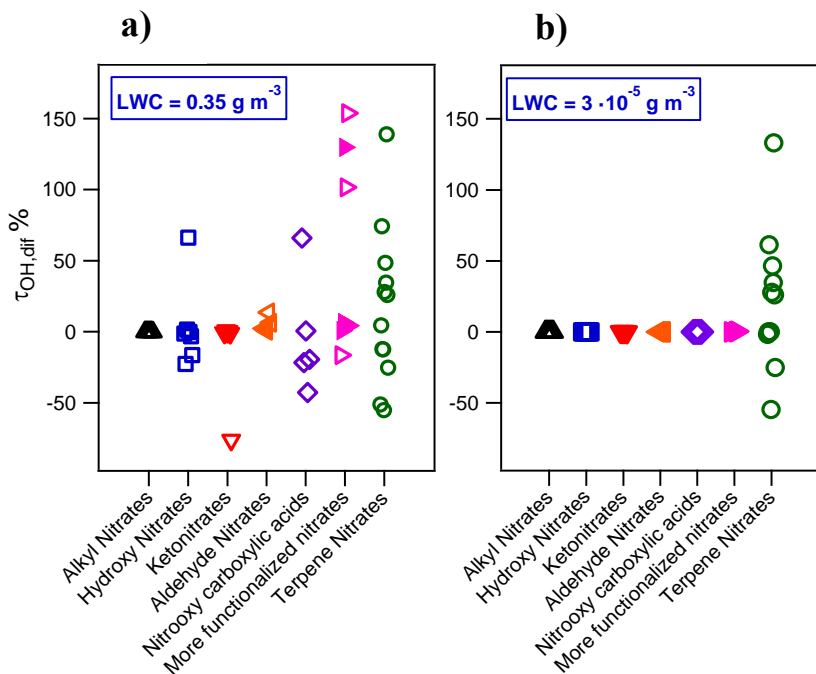


Figure 9: Relative difference of ·OH-oxidation lifetimes between an air parcel with and without liquid water at a) $LWC = 0.35 \text{ g m}^{-3}$ and b) $LWC = 3 \cdot 10^{-5} \text{ g m}^{-3}$ for atmospherically relevant organic nitrates. Filled markers represent organic nitrates derived from isoprene.